Cell Reports

Article

Active Lysogeny in *Listeria Monocytogenes* Is a Bacteria-Phage Adaptive Response in the Mammalian Environment

Graphical Abstract

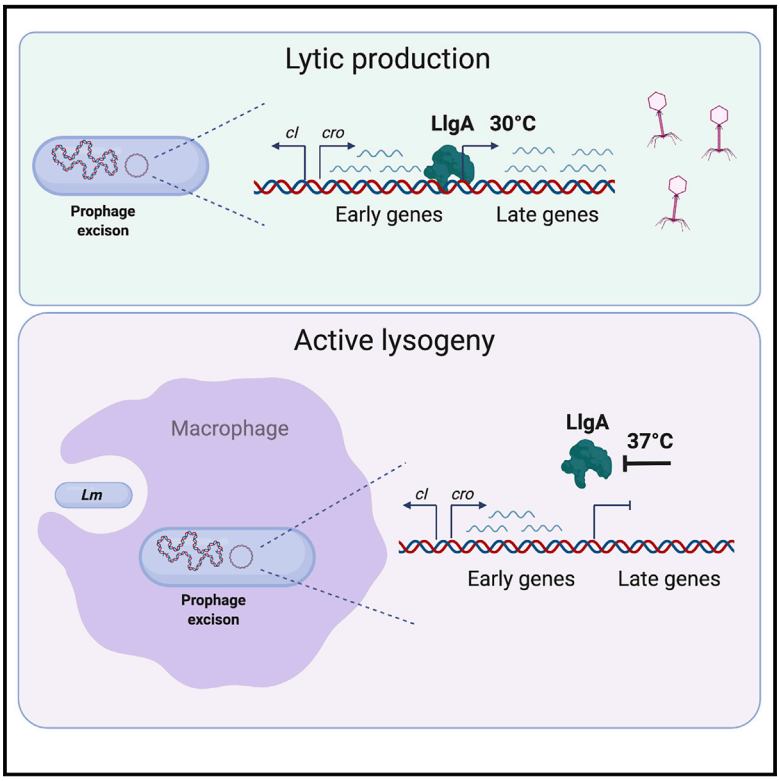

Authors

Anna Pasechnek, Lev Rabinovich, Olga Stadnyuk, ..., Ilya Borovok, Nadejda Sigal, Anat A. Herskovits

Correspondence

anathe@tauex.tau.ac.il

In Brief

Pasechnek at al. describe a phage transcriptional response that supports the pathogenic lifestyle of its host.

Highlights

- *L. monocytogenes* strain 10403S harbors a prophage in its *comK* gene
- During infection of macrophage cells, the prophage lytic pathway is induced
- The phage lytic response is arrested, preventing the expression of the late genes
- LlgA, the late lytic gene activator is specifically inhibited at 37°C

Pasechnek et al., 2020, Cell Reports *32*, 107956
July 28, 2020
https://doi.org/10.1016/j.celrep.2020.107956

CellPress

Cell Reports

CellPress
OPEN ACCESS

Article

Active Lysogeny in *Listeria Monocytogenes* Is a Bacteria-Phage Adaptive Response in the Mammalian Environment

Anna Pasechnek,[1] Lev Rabinovich,[1] Olga Stadnyuk,[1] Gil Azulay,[1] Jessica Mioduser,[1] Tal Argov,[1] Ilya Borovok,[1] Nadejda Sigal,[1] and Anat A. Herskovits[1,2,*]

[1]The School of Molecular Cell Biology and Biotechnology, Faculty of Life Sciences, Tel Aviv University, Ramat Aviv, Tel- Aviv 69978, Israel
[2]Lead Contact
*Correspondence: anathe@tauex.tau.ac.il
https://doi.org/10.1016/j.celrep.2020.107956

SUMMARY

Some *Listeria monocytogenes* (*Lm*) strains harbor a prophage within the *comK* gene, which renders it inactive. During *Lm* infection of macrophage cells, the prophage turns into a molecular switch, promoting *comK* gene expression and therefore *Lm* intracellular growth. During this process, the prophage does not produce infective phages or cause bacterial lysis, suggesting it has acquired an adaptive behavior suited to the pathogenic lifestyle of its host. In this study, we demonstrate that this non-classical phage behavior, named active lysogeny, relies on a transcriptional response that is specific to the intracellular niche. While the prophage undergoes lytic induction, the process is arrested midway, preventing the transcription of the late genes. Further, we demonstrate key phage factors, such as LlgA transcription regulator and a DNA replicase, that support the phage adaptive behavior. This study provides molecular insights into the adaptation of phages to their pathogenic hosts, uncovering unusual cooperative interactions.

INTRODUCTION

Bacteriophages (or phages) are obligatory parasites that exploit bacterial cells for propagation and play a critical role in bacterial evolution. Phages are classified as lytic or lysogenic, based on their infection life cycle (Oppenheim et al., 2005). Upon infection, lytic phages enter a productive cycle, generating infective virions that are liberated via bacterial lysis. In contrast, lysogenic phages utilize various strategies to propagate without activating the lytic cycle. For example, some phages integrate their genome into the bacterial chromosome, turning into prophages that persist in what is considered a phage "dormant state" (Ptashne, 2004). These prophages replicate together with their host chromosome but can switch into lytic production upon exposure to stressful conditions (e.g., DNA damage)—a process termed prophage induction. Even though most bacterial pathogens carry prophages within their genome (Asadulghani et al., 2009; Burns et al., 2015; Figueroa-Bossi et al., 2001; Matos et al., 2013; Ohnishi et al., 2001; Wang et al., 2010), the mechanisms by which they are controlled under the stresses imposed within the mammalian niche remain unclear.

Listeria monocytogenes (*Lm*) is the causative agent of listeriosis disease in humans (Swaminathan and Gerner-Smidt, 2007). It is a Gram-positive, facultative intracellular pathogen that invades a wide array of mammalian cells (Lecuit, 2005). Upon invasion, it resides within a vacuole (or a phagosome), from which it escapes into the host cell cytosol in order to replicate (Barry et al., 1992; Hamon et al., 2006). Most *Lm* strains carry prophages in their genome (e.g., A118, A500, A006, and PSA-like phages) (Dorscht et al., 2009; Klumpp and Loessner, 2013; Zink and Loessner, 1992), yet the impact of these prophages on the pathogenesis of *Lm* is not understood. We previously described an unusual interaction between *Lm* strain 10403S and its prophage ϕ10403S, in which the prophage promotes the virulence of its host via an adaptive behavior (Rabinovich et al., 2012). ϕ10403S is a ~38-kb-long phage of the *Siphoviridae* family that is integrated within the *comK* gene (similar to A118) (Rabinovich et al., 2012). Many *Lm* strains and *Listeria* species carry a prophage within the *comK* gene. To date, over ~8300 *comK*-associated prophages have been sequenced together with their listerial hosts. Owing to the prophage insertion, the listerial *comK* gene was considered non-functional. In *Bacillus subtilis,* ComK functions as the master transcription activator of the competence system (Com), which is known to facilitate the uptake of exogenous DNA (Dubnau, 1999). Noticeably, transcriptome studies of *Lm* 10403S indicated that the *com* genes are highly activated during macrophage infection. Further investigation demonstrated that two major components of the Com system—the Com translocation channel (encoded by *comEC*) and the cell-wall-crossing pseudopilus (encoded by the *comG* operon)—play a role in the escape of *Lm* from the macrophages' phagosomes to the cytosol (Rabinovich et al., 2012). Expression of the *com* genes during *Lm* intracellular growth was found to require the formation of an intact *comK* gene via precise excision of ϕ10403S-prophage. Prophage excision was found to be highly induced in bacteria that are located within

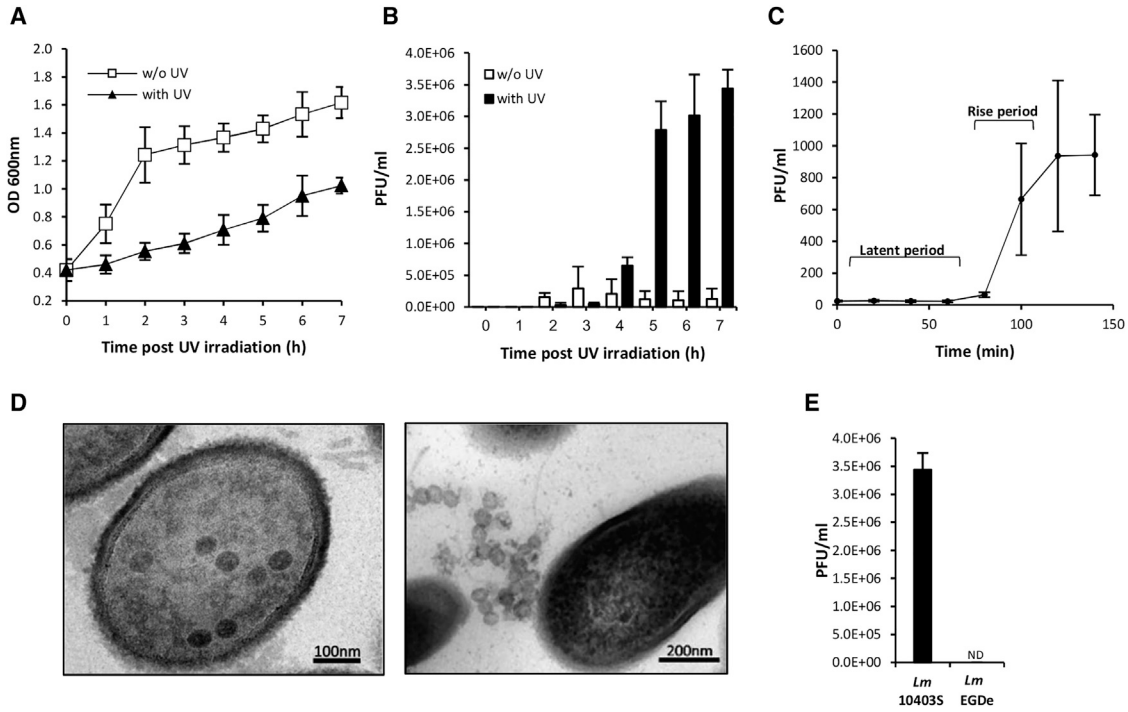

Figure 1. ϕ10403S Lytic Production

(A) Growth analysis of *Lm* 10403S in BHI medium with and without UV irradiation. Cultures were grown for 3 h in BHI to mid-log phase and then irradiated with UV light (at 4 J/cm^2) and incubated at 30°C. Optical density (OD_{600}) measurements were taken every hour as indicated. The data represent a mean of three independent experiments. Error bars represent the standard deviation.

(B) A plaque-forming assay detecting the formation of infective phages after UV irradiation (shown as plaque-forming units, PFUs). The data represent a mean of three independent experiments. Error bars represent the standard deviation.

(C) One-step growth analysis of ϕ10403S lytic infection. Free virion particles of ϕ10403S were used to infect exponentially grown *Lm* bacteria lacking the *comK* gene. Virion production was assayed as PFUs at the indicated time points. The data represent the mean of three independent experiments. Error bars represent the standard deviation.

(D) Transmission electron microscopy of *Lm* 10403S at 4 h post-UV irradiation. Representative images of three independent biological experiments.

(E) A plaque-forming assay detecting the formation of infective phages upon UV irradiation (shown as PFUs) of *Lm* 10403S and EGDe strains grown at 30°C. The data represent the mean of three independent experiments. Error bars represent the standard deviation. ND, not detected.

macrophages' phagosomes, yet unlike classic prophage excision, this did not lead to the production of progeny virions and bacterial lysis (Rabinovich et al., 2012). These findings indicated that during mammalian cell infection, the prophage functions as a DNA molecular switch that regulates *comK* gene expression to support *Lm* intracellular growth. We termed this adaptive phage behavior active lysogeny, representing cases where phages regulate bacterial gene expression via genomic excision without triggering the lytic cycle (Argov et al., 2017a; Feiner et al., 2015). The current study was designed to investigate the molecular mechanisms that uphold ϕ10403S active-lysogenic behavior in macrophage cells. We analyzed the phage genome and transcriptional response under lysogenic, lytic, and active lysogenic conditions and characterized its regulatory and lytic genes. The results uncovered that ϕ10403S acquired a non-classical transcriptional response that supports the survival of its host in the intracellular niche. This finding led to the identification of phage-encoded factors that promote active lysogeny (e.g., factors that facilitate phage excision and re-integration) and a transcriptional regulator that plays a critical role in this bacteria-phage cooperative interaction. The findings presented here demonstrate that in nature, phages have evolved to acquire innovative responses that are beyond the classic lysogenic and lytic, which can support bacteria-phage cooperation under certain circumstances, such as within the mammalian niche.

RESULTS

ϕ10403S-Prophage Switches into Lytic Production in Response to UV Irradiation

To gain a better understanding of the interaction between *Lm* strain 10403S and its prophage ϕ10403S, we first investigated the phage response to conditions that induce the lytic cycle (i.e., conditions that cause DNA damage and trigger the SOS response). Bacteria were grown in the rich brain heart infusion (BHI) medium and exposed to ultraviolet (UV) radiation (4 J/cm^2), a treatment that is known to trigger phage induction (Lamont et al., 1989). Both bacterial growth and infective virion production were monitored following UV irradiation, the latter by using a plaque forming assay. As shown in Figure 1, the UV treatment inhibited the growth of *Lm* bacteria compared to the control (i.e., non-treated bacteria) (Figure 1A). Infective phages

appeared at 4 h post-UV irradiation (liberated via bacterial lysis), reaching a maximum number of ~3.5 × 10^6 plaque-forming units per milliliter of culture (PFUs/ml) (Figure 1B). Of note, mitomycin C, another agent that causes DNA damage, was found to be more potent, yielding 10^8 to 10^9 PFUs/ml (Table S1). To evaluate the burst size of ϕ10403S-phage, a classic one-step growth experiment was performed by infecting *Lm* bacteria, which are lacking the phage and the *comK* gene (Δ*comK*), with free ϕ10403S-phage particles. The results indicated the phage latent period to be ~80 min, the rise period to be ~40 min, and the phage burst size to be ~40 virions per cell (Figure 1C). Examining virion production using transmission electron microscopy revealed phage capsids of ~60 nm inside the bacteria, as well as free phage particles at 4 h post-UV irradiation (Figure 1D). Notably, comparing the lytic production of ϕ10403S to that of a related *comK*-phage of *Lm* strain EGDe revealed that in contrast to ϕ10403S, the EGDe *comK*-phage fails to produce infective phages in response to UV irradiation (Figure 1E). Under mitomycin C treatment, the EGDe phage produced ~10 to 50 PFUs/ml, whereas ϕ10403S produced >10^8 PFUs/ml (Table S1). Taken together, these experiments characterize the lytic response of ϕ10403S upon induction and infection, establishing the basis for further investigation of its response in macrophage cells.

ϕ10403S Lysogenic and Lytic Transcriptional Responses

To study ϕ10403S behavior during *Lm* infection of macrophage cells, we sought to analyze its transcriptional response within the intracellular niche. For this purpose, we first analyzed the phage transcription profile under lysogenic and lytic conditions, using strand-specific RNA sequencing (RNA-seq) analysis. Fifty-two active open reading frames (ORFs) were identified (out of the 54 annotated ORFs) as well as three putative non-coding RNAs (*lasRNA*, *rli140*, and *rliG*) (Toledo-Arana et al., 2009) (Table S2). We could assign a putative function to ~60% of the phage ORFs, while the rest had no homology to known proteins or functional domains (Table S2). We found the ϕ10403S genome to be generally organized in five modules: immunity/integration, lysogeny-lysis switch, early genes (mediating gene regulation and DNA replication), late genes (mediating phage DNA packaging, capsid and tail formation, and bacterial lysis), and lastly, "accessory" genes, whose function is unknown (Figure 2A). Notably, the lysogeny-lysis switch was similar to that of λ-phage, harboring two oppositely directed promoters transcribing *cI*-like and *cro*-like repressor genes (*LMRG_01514* and *LMRG_01515*, respectively) (Johnson et al., 1981; Little et al., 1999; Ptashne, 2004).

ϕ10403S transcriptome analysis under lysogeny indicated that most of the phage genes are repressed, except for a few accessory genes (*LMRG_01555-01556*, *LMRG_01558-01559*) and two putative non-coding RNAs (*lasRNA* and *rliG*) for which the function is unknown (Figure 2B; Table S3). As expected, the phage CI-like repressor and its downstream genes, including the integrase gene (*LMRG_01511* or *int*), were expressed under lysogeny (Figure 2B). Under lytic conditions (i.e., UV irradiation), the phage early and late genes, including the *cro*-like gene, were activated, whereas the *cI*-like repressor gene and its downstream genes were concomitantly repressed (Figure 2C; Table S3). Most of the accessory genes were upregulated under UV irradiation, except for *LMRG_01557*, which was repressed under all tested conditions (Figures 2B and 2C).

To assess the role of the phage genes in the production of infective virions, we generated a library of gene deletion mutants (deleted for one or two genes), which collectively covers the phage genome (32 mutants in total, excluding the phage *cI*-like repressor and functionally redundant genes, such as capsid and tail genes) (Figure 2D). These mutants were subjected to a plaque-forming assay under UV irradiation, and their capacity to produce infective virions was compared to wild-type (WT) bacteria carrying a WT prophage (WT *Lm*) (Figure 2D). The results indicated that most of the phage genes are involved in virion production, but they also identified a number of dispensable genes that encode unknown functions (*LMRG_02918*, *01516*, *lasRNA*, *02984*, *01527*, *02921*, *rliG*, *01530*, and *01555-1556*). Taken together, these results establish ϕ10403S lysogenic and lytic responses and further identify genes that are essential and non-essential to the lytic cycle.

ϕ10403S Exhibits a Unique Transcriptional Response in Macrophage Cells

Next, we analyzed the transcription profile of ϕ10403S during *Lm* infection of macrophage cells. For this purpose, the NanoString technology was employed, which is based on the hybridization of specific probes (Table S4) (Kulkarni, 2011). Bone-marrow-derived macrophage (BMDM) cells were infected with *Lm* bacteria, and the phage transcription profile was detected at 2, 4, and 6 h post-infection (h.p.i). The dynamics of the phage response during macrophage cell infection was compared to the lytic response under UV irradiation at 1, 2, 3, 4, and 5 h post-treatment. The data revealed a unique phage transcriptional response that is specific to the intracellular niche (Figure 3A; Tables S3 and S5). While there was a gradual activation of the phage early and late genes under UV irradiation, during *Lm* infection of macrophage cells, only the early genes were activated, whereas the late genes were essentially repressed (the latter starting at the *terS* gene that mediates phage DNA-packaging and ending at the *lysin* and *holin* genes that mediate bacterial lysis) (Figures 3A–3C). Notably, the data further demonstrated that the *cro*-like repressor gene was strongly activated under UV irradiation and during macrophage cell infection, overall indicating that the phage is effectively induced under both these conditions (Figures 3A and 3D). These observations demonstrate that ϕ10403S is differentially regulated in the intracellular niche. While it appears that the prophage undergoes lytic induction within macrophages, the lytic pathway is arrested halfway, with no transcription of the late genes and, hence, no production of infective virions and bacterial lysis in the intracellular niche.

Identifying Early Genes That Promote Active Lysogeny

Given the observation that the phage early genes are activated in the intracellular niche, we hypothesized that a number of them may play a role in promoting active lysogeny. Active lysogeny involves the excision and re-integration of ϕ10403S genome from the *comK* gene, thereby controlling its expression (Rabinovich et al., 2012). We previously demonstrated that the phage

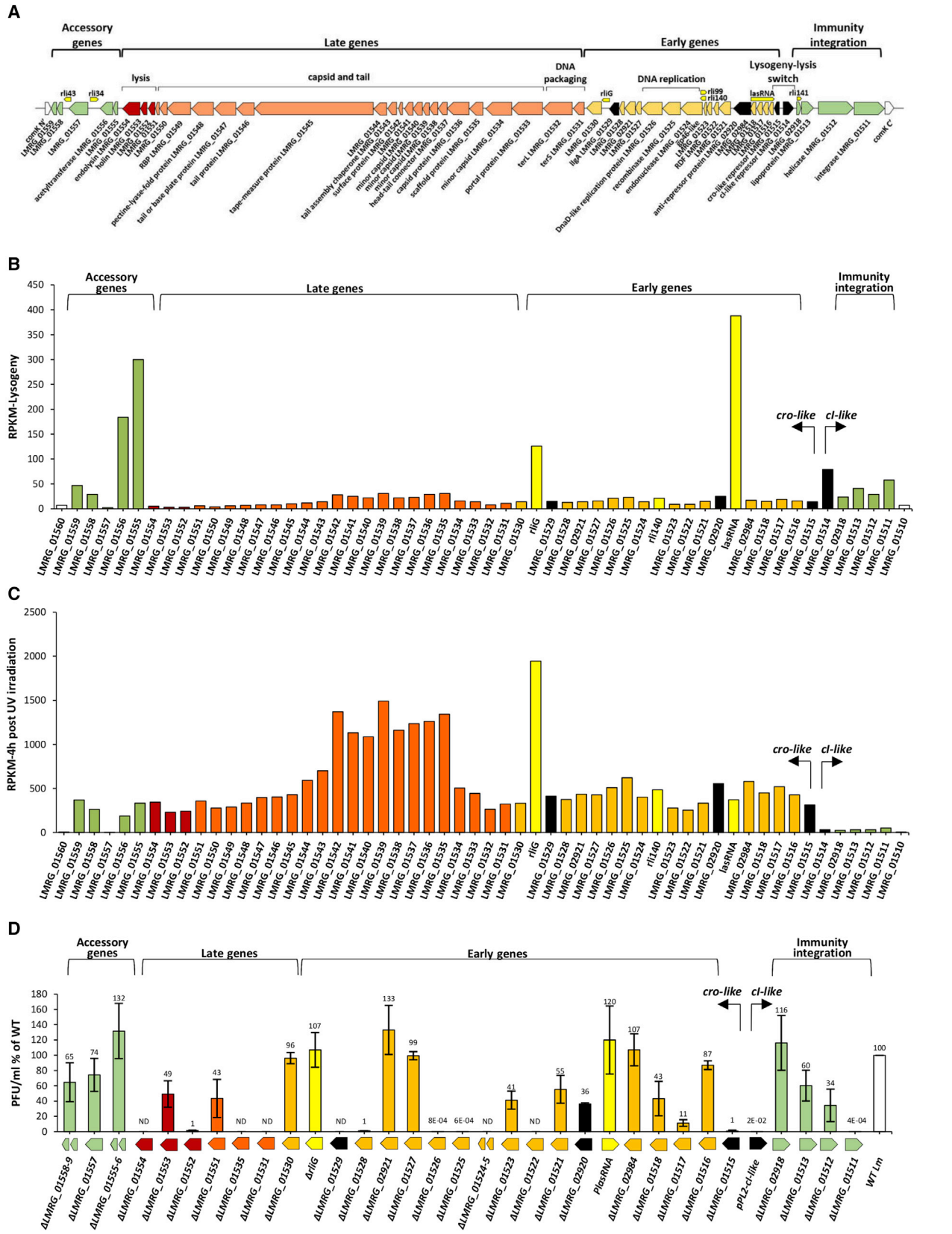

(legend on next page)

integrase (LMRG_01511 or Int) mediates prophage excision, yet many aspects of this process remain unclear, particularly whether the phage-DNA replicates after excision and which factors, if any, facilitate its re-integration into *comK*. Since many of the phage early genes encode proteins predicted to be functionally associated with the phage DNA (e.g., recombinases, a replicase, and an endonuclease; Table S2), we speculated that some of these genes may contribute to the ability of ϕ10403S to function as a DNA-regulatory switch. To address this hypothesis, mutants deleted for each one of the early genes were monitored for phage excision and potential extra-chromosomal replication during *Lm* infection of macrophage cells. Phage DNA excision and extra-chromosomal replication were evaluated by quantifying the number of *attB* and *attP* sites (using qRT-PCR), which are formed only upon phage excision and circularization of its DNA, respectively (Rabinovich et al., 2012). A mutant deleted for the phage integrase gene (Δ*int*) was used as a control, as it fails to excise the chromosome and therefore to replicate as an episome. As expected, in contrast to WT *Lm*, no *attB* or *attP* sites (representing the intact *comK* gene and the circular phage-DNA, respectively) were detected in the intracellularly grown Δ*int* mutant (Figure 4A). Notably, a similar analysis of the early gene mutants detected genes that are important for prophage excision and replication in the intracellular niche. Specifically, a mutant lacking *LMRG_01522* demonstrated a phenotype similar to that of Δ*int*, indicating this gene plays a critical role in ϕ10403S excision (Figure 4A). In accordance with the finding that ϕ10403S excision is a prerequisite for *comK* gene expression and, therefore, the escape of *Lm* from the phagosome to the cytosol, we found Δ*LMRG_01522* mutant to be impaired in phagosomal escape and intracellular growth in macrophage cells (Figures 4B and 4C). Over the course of this study, a homolog of LMRG_01522, Gp44 of A118-phage, was reported to act as a recombination directionality factor (RDF) that activates the phage integrase to promote excision (Mandali et al., 2017). While this finding is in accordance with our observations, it further strengthened the premise that LMRG_01522 plays a critical role in promoting *Lm* phagosomal escape by triggering the formation of an intact *comK* gene during *Lm* infection of macrophages.

Another mutant that exhibited a strong phenotype in the *attP*/*attB* analysis was Δ*LMRG_01526* (Figure 4A). *LMRG_01526* encodes a protein containing a DnaD-like domain, which is a putative replicative DNA-helicase that initiates phage DNA replication. In line with this prediction, intracellularly grown Δ*LMRG_01526* bacteria demonstrated a very low level of *attP* sites in comparison to WT *Lm* (~60-fold less), while the *attB* level was reduced by only 2.5-fold. This finding indicates that ϕ10403S is indeed replicated extra-chromosomally in the intracellular niche. Since the transcriptome data implied that there is no phage DNA packaging into newly formed capsids in the intracellular niche (functions that are encoded by the late genes), we speculated that the extra-chromosomal replication of the phage DNA might be necessary to increase the occurrence of its re-integration into *comK*, thus promoting the phage persistence in the *Lm* chromosome during mammalian infection. To address this hypothesis, we designed a system that monitors the loss of the phage from the *Lm* chromosome during intracellular growth, which is based on the counter selection *pheS** gene. This gene encodes a mutated phenylalanyl-tRNA synthetase that is toxic upon growth in medium supplemented with *p*-chloro-phenylalanine (Argov et al., 2017b). The *pheS** gene was cloned into the phage genome (in the accessory module) and was used to evaluate the emergence of phage-cured bacteria upon *Lm* intracellular growth. We surmised that if the phage DNA fails to re-integrate into *comK*, it will be lost during *Lm* intracellular growth. Using this system, we found that ϕ10403S re-integration into *comK* is a highly efficient process, with a phage-loss rate of 1 in 500,000 bacteria (using WT *Lm* carrying a WT phage) (Argov et al., 2019). Notably, performing this analysis using a Δ*LMRG_01526* mutant, we found it to exhibit a phage-loss rate of 1 in 30,000 bacteria, which is 15-fold greater than WT bacteria (Figure 4D). A similar phenotype was observed upon intravenous mice infections. Monitoring phage-cured bacteria 48 h post-mice infection revealed that the number of phage-cured bacteria recovered from the livers of mice infected with Δ*LMRG_01526* was greater than ~30-fold the number recovered using WT *Lm* (Figure 4E). These findings indicate that phage DNA replication in the intracellular niche contributes to phage re-integration into *comK*, hence promoting its persistence within the *Lm* chromosome during infection of mammalian cells. Altogether, these findings provide an insight into the fate of ϕ10403S within the mammalian niche and further explain the activation of the early genes in this environment.

Characterizing ϕ10403S Main Transcription Regulators

Having discovered that the transcription of the late genes is specifically blocked during *Lm* infection of macrophage cells, we next aimed to identify the phage regulator(s) that control the phage late genes. To this end, we identified four putative regulatory proteins in the ϕ10403S-genome. Among these are CI and Cro-like repressors and two additional regulators: LMRG_02920 and LMRG_01529, which encode for a putative

Figure 2. ϕ10403S Transcriptional Response under Lysogenic and Lytic Conditions

(A) Schematic representation of the ϕ10403S-genome including predicted genes and functional modules. Regulatory genes are marked in black, ncRNAs are marked in bright yellow, immunity/integration and accessory genes are marked in green, early genes are marked in orange, late genes are marked in peach, and lysis genes are marked in red.

(B) Strand-specific RNA-seq analysis of ϕ10403S under lysogenic conditions (i.e., bacteria grown in BHI to exponential phase at 30°C). Transcription levels are indicated as RPKM (scaled reads per kilobase per million reads). Data represent the mean of three independent experiments.

(C) Strand-specific RNA-seq analysis of ϕ10403S-phage under lytic conditions (4 h post-UV irradiation). Transcription levels are indicated as RPKM. Data represent the mean of three independent experiments.

(D) A plaque-forming assay detecting the formation of infective phages upon UV irradiation of *Lm* 10403S and indicated phage mutants grown at 30°C, as well as a strain overexpressing CI-like repressor (pPL2-*cI*-like). Data are presented as a percentage relative to the levels observed in WT *Lm*. Data represent a mean of three independent experiments. Error bars represent the standard deviation. ND, not detected.

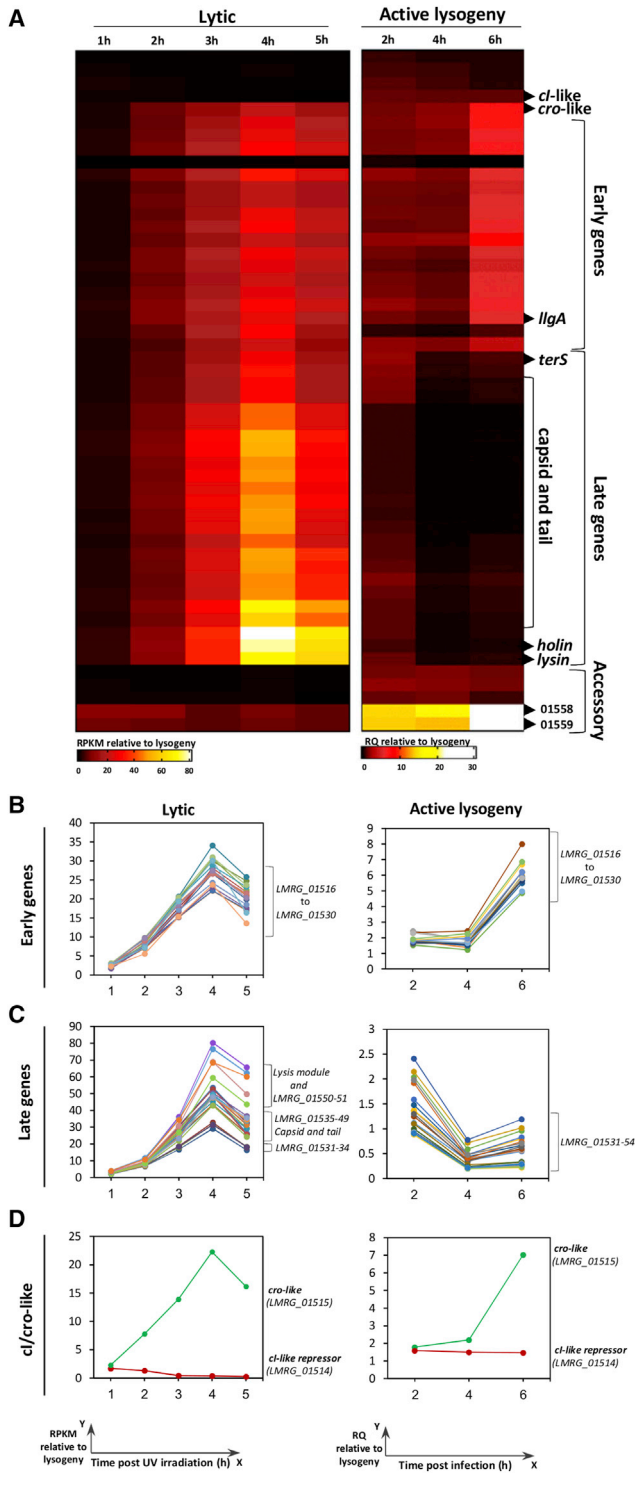

Figure 3. ϕ10403S Transcriptional Response in Macrophage Cells

(A) ϕ10403S transcriptional response under UV irradiation and active lysogenic conditions, the latter during *Lm* infection of BMDM cells. Strand-specific RNA-seq analysis under UV irradiation was performed by Illumina. Transcription analysis during active lysogeny was performed using nCounter analysis. Transcription levels are presented as relative counts, compared to the levels observed in the lysogenic state (i.e., bacteria grown exponentially in BHI medium at 30°C). Data represent the mean of three independent experiments.

(B–D) Transcription profile of ϕ10403S (B) early genes, (C) late genes, and (D) regulatory genes under lytic and active lysogenic conditions.

anti-repressor and an ArpU-like transcription regulator, respectively (Quiles-Puchalt et al., 2013) (Figure 2A). Mutants deleted for each of these regulatory genes (except for the *cI*-like repressor gene) were severely impaired in the production of infective virions under UV irradiation (Figure 2D). Of note, deletion of the *cI*-like gene could not be achieved because it results in the immediate induction of the phage and bacterial lysis. To validate the role of the CI-like repressor as the main phage repressor, we overexpressed it using a constitutive promoter from the integrative pPL2 plasmid (pPL2-*cI-like*) and examined its ability to repress virion production under UV irradiation. As predicted, overexpression of the CI-like repressor blocked the production of infective virions, validating its function as the main phage repressor that maintains lysogeny (shown in Figure 2D; pPL2-*cI*-like). To examine the function of the other regulators, we analyzed their effect on the transcription of early and late genes using qRT-PCR (Figure 5). Bacterial mutants deleted for each regulatory gene were subjected to UV irradiation, and total RNA was extracted before (time 0) and at 1, 3, and 5 h post-UV irradiation. Performing this analysis confirmed that LMRG_01515 is a classic Cro-like repressor, which represses the transcription of the early genes in the course of the lytic pathway (including *LMRG_02920* and *LMRG_01529*) (Figure 5A). The function of the putative anti-repressor LMRG_02920 was less definitive. A mutant lacking this gene exhibited an increase in the transcription of the early genes and a decrease in the transcription of the late genes at later time points (4 to 5 h post-UV), suggesting it may temporally regulate the transcription of the early and late genes in the course of the lytic pathway (Figure 5B). Analyzing the LMRG_01529 putative regulator, we found that it functions as the main activator of the late genes. A mutant deleted of *LMRG_01529* failed to transcribe the late genes, whereas the early and regulatory genes were transcribed at levels similar to those in WT *Lm* harboring a WT phage (Figure 5C). We therefore named LMRG_01529 LlgA (late-lytic gene activator of ϕ10403S).

LlgA Protein Activity Is Inhibited in the Intracellular Niche

Given our finding that LlgA is the activator of the late genes, we speculated that it may be specifically inhibited in the intracellular niche. The transcriptome data indicated that *llgA* is transcribed within the macrophages together with the early genes, and yet the late genes are not expressed (Figure 3A). This observation implies that LlgA is inhibited post-transcriptionally, possibly during translation or even later, at the protein level. To examine these possibilities, a six-histidine-tag was fused to the carboxy-terminus of LlgA (in the prophage genome), and western blot analysis was performed to detect the level of LlgA proteins in intracellularly grown bacteria. No LlgA proteins were detected in intracellular bacteria, yet we cannot conclude that LlgA is not translated, as many listerial proteins are hard to detect in

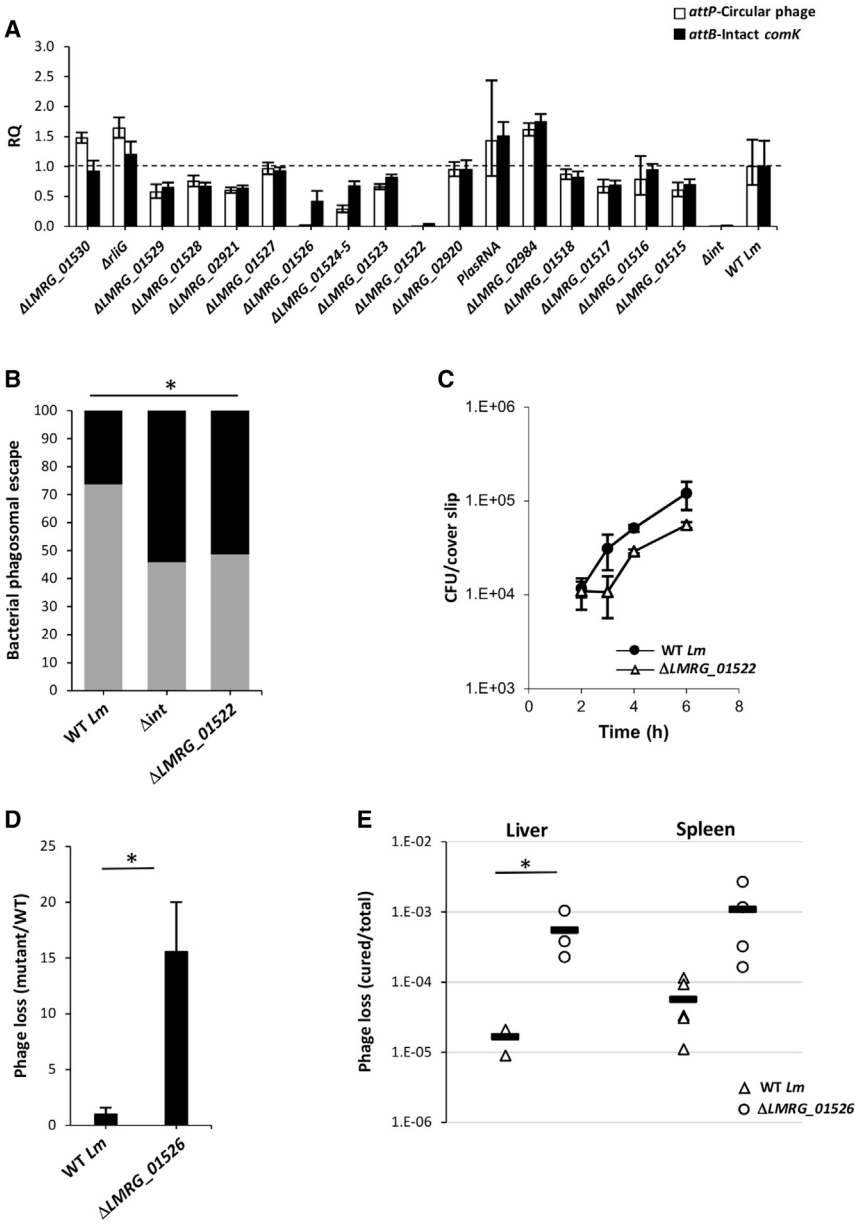

Figure 4. Phage Early Genes That Contribute to Active Lysogeny

(A) qRT-PCR analysis of *attB* and *attP* sites in WT *Lm* and indicated mutants grown in BMDM cells for 6 h. Data are presented as relative quantity (RQ), compared to the levels in WT bacteria. The data represent a mean of three independent experiments. Error bars indicate the 95% confidence interval.

(B) A bacterial phagosomal escape assay. Percentage of bacteria that escaped the macrophage phagosomes as determined by a microscope fluorescence assay. Macrophages were infected with WT *Lm* and Δ*LMRG_01522*, as well as with Δ*int* as a control. The data represent two biological repeats. *$p < 0.05$ as calculated by the χ-test.

(C) Intracellular growth of WT *Lm* and Δ*LMRG_01522* mutant in BMDM cells. The data are representative of three independent experiments. Error bars represent the standard deviation of a triplicate.

(D) Analysis of phage loss in Δ*LMRG_01526* mutant in comparison to WT *Lm* grown in macrophage cells for 6 h. The number of phage-cured bacteria isolated from macrophages infected with *ΔLMRG_01526* mutant was normalized to that of WT bacteria. The data represent the mean of three independent experiments. Error bars represent the standard deviation. *$p < 0.05$ as calculated by Student's t test.

(E) Analysis of phage loss in the Δ*LMRG_01526* mutant in comparison to WT *Lm* during *in vivo* infection of C57BL/6 mice (48 h.p.i.). The number of phage-cured bacteria isolated from the spleens and livers of infected mice was normalized to the total number of bacteria recovered. The data represent 3 to 5 mice per sample. *$p = 0.05$ as calculated by Student's t test.

macrophage cells due to their relatively low levels. As an alternative approach, we examined the impact of LlgA overexpression on intracellularly grown bacteria by expressing it from pPL2 plasmid using the promoter of the *actA* virulence gene, which was shown to be highly activated intracellularly (pPL2-P*actA*-*llgA*) (Reniere et al., 2016). Remarkably, LlgA expression resulted in the immediate killing of the bacteria within the macrophage cells. This killing was driven by the phage lysis proteins (holin and lysin), as bacteria that were cured of the phage or deleted of the lysis genes (Δϕ-pPL2-P*actA*-*llgA* and Δ(*lysis*)$_\phi$-pPL2-P*actA*-*llgA*, respectively) grew similarly to WT *Lm* in the macrophage cells (Figure 6A). This observation supports the premise that LlgA is inhibited in the intracellular niche, in order to prevent the activation of the late lytic genes.

A clue to the mode of regulation of LlgA within the intracellular niche came from *in vitro* experiments designed to investigate LlgA translation and protein activity. For this purpose, *llgA-his*-tagged (*llgA-his*) was cloned into the pPL2 plasmid, this time under the regulation of an inducible tetracycline repressor (TetR) dependent promoter (pPL2-P*tetR*-*llgA-his*). Monitoring the growth of LlgA-expressing bacteria (WT *Lm*-pPL2-P*tetR*-*llgA-his*) in BHI medium without UV irradiation unexpectedly revealed that the bacteria failed to grow at 30°C but did grow at 37°C, as compared to WT *Lm* not carrying the *llgA* plasmid (this phenotype was observed without the addition of a TetR inducer) (Figures 6B and 6C). Interestingly, similarly to the LlgA-mediated bacterial killing observed in macrophages, the lack of bacterial growth at 30°C was entirely attributed to the triggering of bacterial lysis by the phage lysis proteins. A mutant deleted for the phage lysis genes harboring pPL2-P*tetR*-*llgA-his* (Δ(*lysis*)$_\phi$-pPL2-P*tetR*-*llgA-his*) grew similarly to WT bacteria at both 30°C and 37°C (Figures 6B and 6C). While these findings demonstrated that ectopic expression of LlgA is sufficient to activate

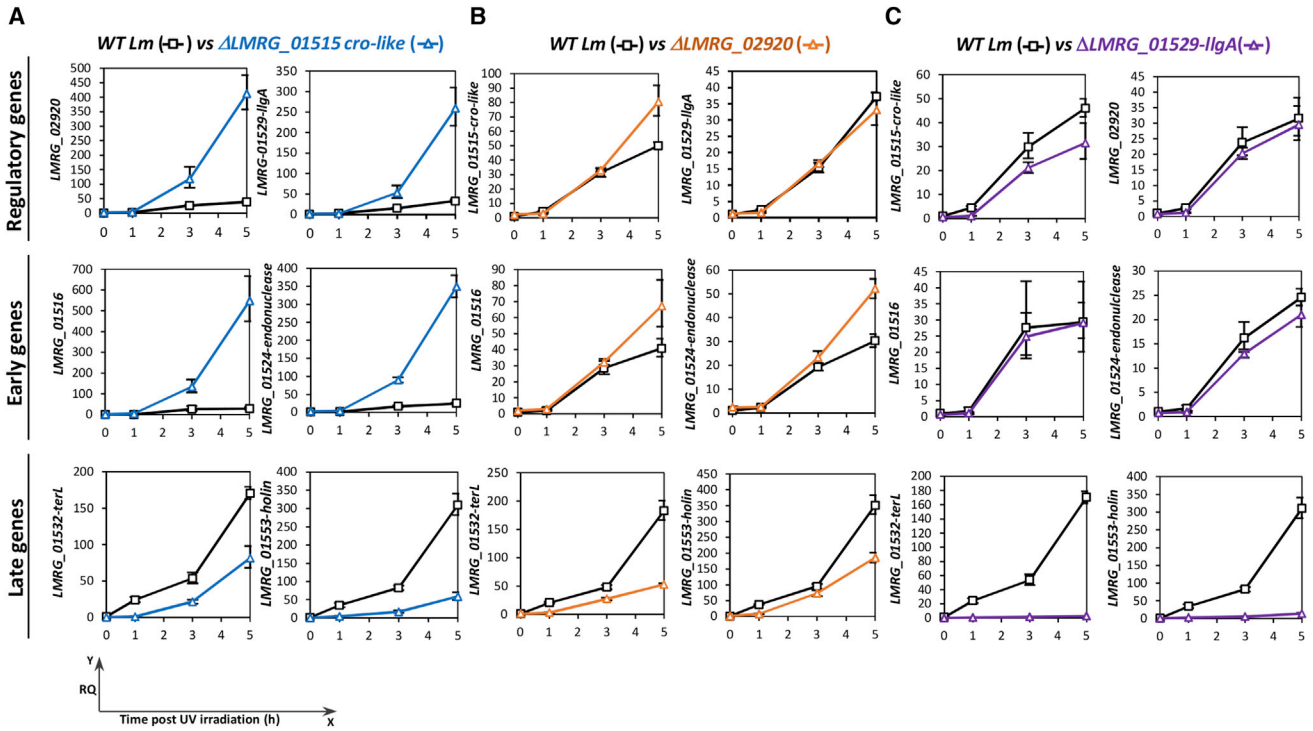

Figure 5. Characterization of ϕ10403S Regulatory Proteins

qRT-PCR analysis of selected phage genes representing the early gene module (*LMRG_01516* and *LMRG_01524-endonuclease*), the late gene module (*LMRG_01532-terL* and *LMRG_01553-holin*), and the putative regulatory genes (*LMRG_01515*, *LMRG_02920*, and *LMRG_01529*) in WT *Lm* and regulatory gene mutants as indicated.

(A) Analysis of genes regulated by *LMRG_01515*.

(B) Analysis of genes regulated by *LMRG_02920*.

(C) Analysis of genes regulated by *LMRG_01529*.

RNA was isolated from bacteria grown in BHI medium at 30°C after UV irradiation at the indicated time points. The data are representative of three independent experiments. Transcription levels are presented as a RQ, compared to their levels in WT bacteria prior to UV irradiation, indicated as t = 0. Error bars indicate the 95% confidence interval of the triplicate.

the expression of the late genes even in the absence of UV irradiation, they further revealed that LlgA is preferentially inhibited under 37°C, which is the temperature of the intracellular niche. Of note, increasing the expression of LlgA by the addition of the TetR inducer anhydrotetracycline (AT) resulted in bacterial killing also at 37°C, demonstrating that a high level of LlgA can override its temperature-dependent inhibition (as observed in intracellularly grown bacteria overexpressing LlgA) (Figures 6B and 6C). To further investigate the observed temperature-dependent regulation of LlgA, we compared its mRNA and protein levels in bacteria grown at 30°C and 37°C (without UV irradiation), as well as its ability to activate the transcription of early and late genes. LlgA transcription and translation were assessed in a phage-cured strain or a strain deleted of the phage lysis genes (Δϕ or Δ(*lysis*)$_{\phi}$) in order to avoid unwanted bacterial lysis and therefore the loss of mRNA and proteins. Interestingly, both qRT-PCR and western blot analyses indicated that *llgA* is transcribed and translated equally well at 30°C and 37°C (Figures 6D and 6E). However, the late genes were preferentially activated only at 30°C and not at 37°C (Figure 6F). As expected, the early genes remained repressed at both temperatures, since the phage lysogeny-lysis switch is not induced in the absence of UV irradiation, and hence the early genes are not activated (Figure 6F). The results of these experiments suggest that the activity of LlgA is thermo-regulated (i.e., active at 30°C and less active at 37°C), which is in line with the phage transcriptional response in the intracellular niche (Figure 3A). To examine whether LlgA thermo-regulation is mediated by another phage-encoded factor, we constructed a reporter system for LlgA activity and tested it in *Lm* bacteria lacking the prophage (Δϕ). To this end, the *terS* gene, which is positively regulated by LlgA, was cloned with its upstream region (including LlgA putative binding sites) into pPL2 plasmid that carries *llgA* under TetR regulation (pPL2-P*tetR-llgA-terS*). The plasmid was then introduced into Δϕ bacteria, and, using qRT-PCR, the transcription levels of *terS* and *llgA* were evaluated during growth at 30°C and 37°C. The data indicated that LlgA thermo-regulation does not involve other phage factors, as the *terS* gene was preferentially activated at 30°C and less so at 37°C, even in the absence of the prophage (Figure 6G). Of note, *llgA* transcription from the pPL2 plasmid was comparable under both temperatures. To examine whether a listerial factor is responsible for the observed LlgA

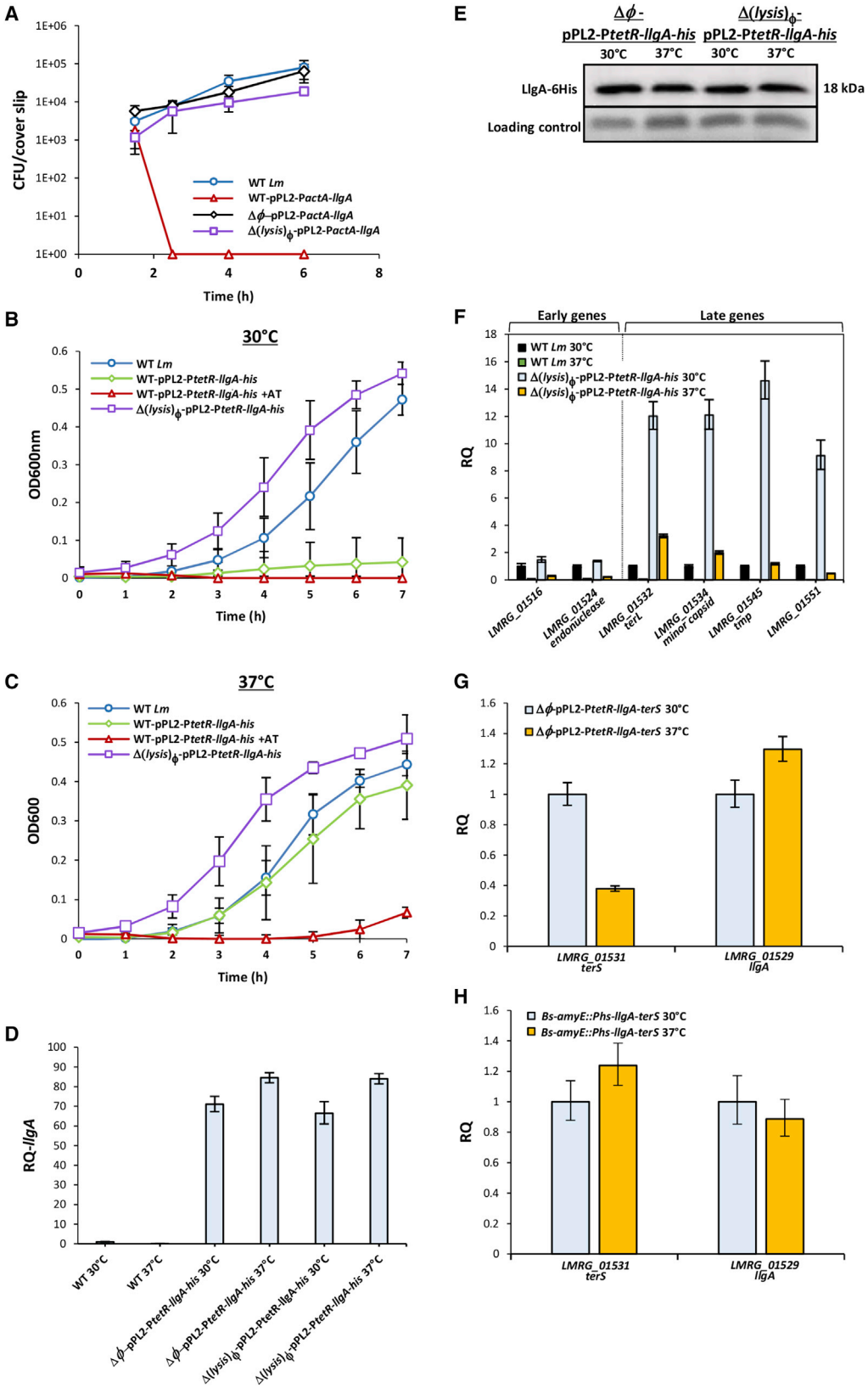

(legend on next page)

thermo-regulation, we introduced the *llgA-terS* reporter system to *Bacillus subtilis* bacteria. The *llgA gene* was cloned under the regulation of the hyperspank promoter (P*hs*), and the entire P*hs-llgA-terS* cassette was integrated into the *B. subtillis* chromosome (in the *amyE* gene) using AES777 plasmid (*amyE*::P*hs-llgA-terS*). The bacteria were then grown in Luria Bertani (LB) medium at 30°C and 37°C (with the addition of isopropyl β-d-1 thiogalactopyranoside [IPTG]), and the transcription levels of *terS* and *llgA* were evaluated. Interestingly, we found the *terS* gene to be equally transcribed under both temperatures, suggesting that LlgA thermo-regulation is mediated by a listerial specific factor that is absent in *B. subtilis* (Figure 6H). Although further attempts to identify this presumably existing listerial factor were not successful, the findings presented here indicate that LlgA is a critical factor in the interaction of *Lm* with its inhabiting prophage in the mammalian environment.

DISCUSSION

Lysogeny was first described in 1925 with the observation that some bacterial strains lyse and produce infective virions (Lwoff, 1953). D'Herelle, who also observed this phenomenon, suggested that these strains are "symbiotic," maintaining mutualistic interactions with their phages (Lwoff, 1953). Since then, a number of bacteria-phage symbiotic interactions have been documented, describing cases where lysogenic phages provide immunity to their hosts (superinfection exclusion) as well as virulence or metabolic genes (lysogenic conversion) (Bondy-Denomy et al., 2016; Brüssow et al., 2004; Waldor and Friedman, 2005). Since under lysogeny, the bacteria and the phage become a single genetic unit, a unique situation is formed in which their interests are temporarily aligned. Within this context, innovative and complex interactions evolve that balance the bacteria and the phage needs, sometimes leading to cooperative behaviors under certain circumstances. In line with this premise, the results of this study describe an example of a bacteria-phage interaction in which non-classical phage transcriptional regulation and molecular adaptations operate to promote bacteria-phage cooperation in the intracellular environment.

This study relies on our previous observation that the *Lm* ϕ10403S-prophage acts as a molecular switch to regulate *comK* gene expression during *Lm* infection of macrophage cells. While this finding suggested that the phage had acquired an adaptive behavior aligned to the pathogenic lifestyle of its host, the underlying mechanisms and molecular adaptations that uphold this interaction were unknown. In this study, we comprehensively investigated the ϕ10403S genome, transcriptional responses, and regulatory proteins, revealing a unique transcription profile and key factors that collectively control the phage active lysogenic behavior in mammalian cells. We characterized the lytic production of ϕ10403S under UV irradiation and upon phage infection, and we found the phage to be functional, producing dozens of infective virions per cell. Interestingly, we further found that this characteristic is not necessarily shared by all listerial *comK*-phages: for example, the *comK*-phage of *Lm* strain EGDe hardly produced infective virions in response to SOS, suggesting that it has evolved differently.

Characterizing the transcription profile of ϕ10403S under lysogenic and lytic conditions, we identified 52 active ORFs and 3 putative ncRNAs. The data demonstrated that during lysogeny, most of the phage genes are repressed, yet the data also identified a number of genes that are highly expressed during lysogeny that require further investigation (*lasRNA*, *rliG*, *LMRG_01555*, *01556*, *01558*, and *01559*). Notably, four of these genes are located in the accessory gene module, suggesting that they possess functions that benefit the bacteria and/or the phage under lysogeny. For example, the "accessory" gene module of related *Listeria* phages has been shown to encode for anti-CRISPR proteins (Acrs) that target the type II CRISPR-Cas system of *Lm* (Osuna et al., 2019; Rauch et al., 2017). These proteins were shown to function under lysogeny and less upon lytic infection, suggesting they have been evolved to protect the bacteria and the phage under this condition. Under UV irradiation, we found the ϕ10403S lysogeny-lysis switch to be induced, resulting in the robust activation of the phage early and late lytic genes.

Figure 6. LlgA Activity Is Thermo-Regulated

(A) Intracellular growth analysis of WT *Lm* and mutants that are cured of the phage (Δϕ) or deleted of lysis genes (Δ(*lysis*)$_{\phi}$) expressing *llgA* (pPL2-P$_{actA}$-*llgA*) in BMDM cells. Data are representative of three independent experiments. Error bars represent the standard deviation of a triplicate.

(B and C) Growth analysis of WT *Lm* and bacteria expressing *llgA-his* from a TetR-dependent promoter (pPL2-P$_{tetR}$-*llgA-his*), as well as a mutant deleted of the phage lysis genes (Δ(*lysis*)$_{\phi}$) harboring pPL2-P$_{tetR}$-*llgA-his* with and without the addition of anhydrotetracycline (AT) at (B) 30°C and (C) 37°C. Data represent the mean of three independent experiments. Error bars represent the standard deviation.

(D) qRT-PCR analysis of *llgA* transcription levels at 30°C and 37°C in WT *Lm* and in Δ(*lysis*)$_{\phi}$ and Δϕ strains harboring pPL2-P$_{tetR}$-*llgA-his*. Transcription levels are presented as a RQ, compared to the levels in WT bacteria grown at 30°C. mRNA levels were normalized to the levels of 16S rRNA. The data are representative of three independent experiments. Error bars indicate the 95% confidence interval.

(E) Western blot analysis of LlgA-6His protein obtained from WT *Lm* grown at 30°C and 37°C and from Δ(*lysis*)$_{\phi}$ strain and a strain cured of the phage Δϕ, all harboring pPL2-P$_{tetR}$-*llgA-his*. Equal amounts of total protein were separated on a 15% SDS-PAGE that was blotted and probed with anti-6His antibody. The experiment was performed three times, and the figure shows a representative blot. Coomassie staining was used as a loading control (lower panel)

(F) qRT-PCR analysis of selected phage genes, representative of the early and late gene modules in WT *Lm* and in Δ(*lysis*)$_{\phi}$ mutant harboring pPL2-P$_{tetR}$-*llgA-his* grown in BHI at 30°C and 37°C. Transcription levels are presented as a RQ, compared to the levels in WT bacteria grown at 30°C. mRNA levels were normalized to the levels of 16S rRNA. The data are representative of three independent experiments. Error bars indicate the 95% confidence interval.

(G) qRT-PCR analysis of *terS* and *llgA* genes expressed from the pPL2 plasmid (pPL2-P$_{tetR}$-*llgA-terS*) in *Lm* bacteria that are cured of the phage (Δϕ) grown in BHI at 30°C and 37°C. Transcription levels are presented as a RQ, compared to the levels in bacteria grown at 30°C. mRNA levels were normalized to the levels of 16S rRNA. The data are representative of three independent experiments. Error bars indicate the 95% confidence interval.

(H) qRT-PCR analysis of *terS* and *llgA* genes expressed from *amyE*::P$_{hs}$-*llgA-terS* in *B. subtillis* bacteria grown in LB at 30°C and 37°C with IPTG. Transcription levels are presented as a RQ, compared to the levels in bacteria grown at 30°C. mRNA levels were normalized to the levels of 16S rRNA. The data are representative of three independent experiments. Error bars indicate the 95% confidence interval.

Systematic analysis of the phage genome indicated that most of the genes are involved in the production of infective virions, whereas some are completely dispensable. Intriguingly, the dispensable genes were found to be distributed across the whole phage genome. This observation relates to one of the greatest mysteries in phage research that is the remarkably large reservoir of unknown genes found in phage genomes, which implies that bacteria-phage interactions in nature are even more complex than currently understood.

The main observation of this study concerns the transcriptional response of ϕ10403S during *Lm* infection of macrophage cells (i.e., active lysogeny). The results indicate that ϕ10403S is induced upon macrophage infection; however, unlike classic phage induction, the lytic pathway is arrested halfway. These findings establish that active lysogeny is a tightly regulated process that prevents the formation of infective virions and bacterial lysis within the intracellular niche. Further, we found that this unique transcriptional response supports the phage function as a DNA regulatory switch (regulating *comK* gene), which is designed to facilitate *Lm* phagosomal escape and intracellular growth. Within the early gene module, we identified genes that mediate prophage excision and re-integration, thus playing an important role in *comK* regulation. The data support the premise that LMRG_01522 functions as an RDF that activates prophage excision and that LMRG_01526 functions as a replicative factor that mediates the phage DNA replication. We found that upon excision, the phage DNA is replicated in the intracellular niche as an episome, and this replication increases the chances of its re-integration into *comK*. Bacteria carrying a mutated phage that fails to replicate lost the phage more frequently upon macrophage and mice infections, overall indicating that phage replication plays an important role in the persistence of ϕ10403S within the *Lm* chromosome.

The transcription profile of ϕ10403S during macrophage cell infection revealed that the late genes are specifically repressed in the intracellular niche. This finding corroborated our previous observation that the phage does not produce infective virions or trigger bacterial lysis in the intracellular environment, thereby supporting *Lm* intracellular growth (Rabinovich et al., 2012). Notwithstanding, we recently demonstrated that ϕ10403S is not the only lytic phage element that inhabits the *Lm* chromosome (Argov et al., 2017b). *Lm* 10403S harbors another cryptic phage element that encodes for tail-like bacteriocins named monocins. We found that this monocin element is also activated under UV irradiation and triggers the production and release of monocins via bacterial lysis, independently of ϕ10403S (Argov et al., 2017b, 2019). Interestingly, we also found that ϕ10403S and the monocin element are tightly co-regulated, as they share a common anti-repressor, MpaR, which is a metalloprotease that is encoded by the monocin element. Under SOS stress or infection of mammalian cells, MpaR concomitantly cleaves the CI-like repressors of both elements (ϕ10403S and monocin), thus synchronizing their lytic induction. Further investigation indicated that the lytic genes of the monocin element (including its lysis genes) are also repressed in the intracellular niche, yet the mechanism of their repression is still not clear (Argov et al., 2019). Of note, the monocin element is evolutionarily more ancient than ϕ10403S and hence may have acquired a different mechanism to regulate its lytic genes in the intracellular niche. While the data indicate that LlgA is not involved in the regulation of the monocin genes (Figure 6A), the findings reveal that a controlled inhibition of phage-derived lytic genes (particularly lysis genes) in the intracellular environment is a common mechanism that is essential for the adaptation of prophages (infective and cryptic) to the pathogenic lifestyle of their host.

LlgA belongs to the Ltr super-family of late transcriptional regulators (Quiles-Puchalt et al., 2013). These activators were shown to bind upstream the *terS* gene, which is the first gene of the late gene module. We identified hundreds of LlgA homologs in *Listeria* genomes, located in various *comK* and non-*comK* prophages (e.g., A500 and A006-like phages), many of them exhibiting a remarkable amino acid sequence identity (examples are in Figure S1). Interestingly, overexpression of LlgA immediately triggered a bacterial killing in macrophage cells. This killing was solely dependent on the phage and associated with its lysis proteins, supporting the hypothesis that LlgA is inhibited in the intracellular niche. The phage transcription profile indicated that while *llgA* is transcribed in the intracellular niche, there is no expression of the downstream-regulated late genes, implying that LlgA regulation may be post-transcriptional. Since we could not investigate LlgA translation and activity in the intracellular environment (the LlgA protein was undetectable), we studied LlgA expression from the pPL2 plasmid. The experiments revealed that LlgA directly activates the late genes and thus triggers bacterial lysis, even in the absence of UV irradiation. In addition, further investigation demonstrated that the LlgA protein is preferentially active at 30°C and less active at 37°C, which is the temperature of the intracellular niche. Despite similar levels of transcription and translation at both temperatures, at 37°C, the LlgA protein failed to activate the transcription of the late genes. We found this thermo-regulation of LlgA to be independent of other phage factors, yet possibly reliant on a listerial specific factor, as it was not observed in *B. subtilis*. Taken together, the data point out LlgA as a critical factor in the interaction of *Lm* with its prophage and further suggest that LlgA thermo-regulation has evolved to support the survival of *Lm* (and the phage) in the mammalian host. Finally, this study strengthens the premise that lysogeny is a highly versatile state, in which bacteria and their inhabiting phages are continuously subjected to evolutionary selection (Bobay et al., 2013; Howard-Varona et al., 2017). We posit that like *Lm* and its prophage, many other bacterial pathogens also maintain unique lysogenic interactions with their prophages that are designed to support mutual survival in the mammalian host.

STAR★METHODS

Detailed methods are provided in the online version of this paper and include the following:

- KEY RESOURCES TABLE
- RESOURCE AVAILABILITY
  - Lead Contact
  - Materials Availability
  - Data and Code Availability
- EXPERIMENTAL MODEL AND SUBJECT DETAILS

SUPPLEMENTAL INFORMATION

Supplemental Information can be found online at https://doi.org/10.1016/j.celrep.2020.107956.

ACKNOWLEDGMENTS

We thank Tasneem Bareia and Avigdor Eldar for their help with the *B. subtillis* experiments. This work was funded by European Research Council (ERC) starting and consolidator grants for A.A.H. (Patho-Phage-Host 335400 and Co-Patho-Phage 817842) and an Israel Science Foundation grant for A.A.H. (ISF 1381/18).

AUTHOR CONTRIBUTIONS

A.P. and A.A.H. designed the study. A.P., L.R., O.S., G.A., J.M., T.A., and N.S. performed the experiments. N.S. validated the results. I.B. performed bioinformatic analysis, and A.A.H. prepared the manuscript.

DECLARATION OF INTERESTS

The authors declare no competing interests.

Received: February 7, 2020
Revised: May 5, 2020
Accepted: July 2, 2020
Published: July 28, 2020

REFERENCES

Argov, T., Azulay, G., Pasechnek, A., Stadnyuk, O., Ran-Sapir, S., Borovok, I., Sigal, N., and Herskovits, A.A. (2017a). Temperate bacteriophages as regulators of host behavior. Curr. Opin. Microbiol. *38*, 81–87.

Argov, T., Rabinovich, L., Sigal, N., and Herskovits, A.A. (2017b). An Effective Counterselection System for Listeria monocytogenes and Its Use To Characterize the Monocin Genomic Region of Strain 10403S. Appl. Environ. Microbiol. *83*, e02927-16.

Argov, T., Sapir, S.R., Pasechnek, A., Azulay, G., Stadnyuk, O., Rabinovich, L., Sigal, N., Borovok, I., and Herskovits, A.A. (2019). Coordination of cohabiting phage elements supports bacteria-phage cooperation. Nat. Commun. *10*, 5288.

Asadulghani, M., Ogura, Y., Ooka, T., Itoh, T., Sawaguchi, A., Iguchi, A., Nakayama, K., and Hayashi, T. (2009). The defective prophage pool of Escherichia coli O157: prophage-prophage interactions potentiate horizontal transfer of virulence determinants. PLoS Pathog. *5*, e1000408.

Bareia, T., Pollak, S., and Eldar, A. (2018). Self-sensing in Bacillus subtilis quorum-sensing systems. Nat. Microbiol. *3*, 83–89.

Barry, R.A., Bouwer, H.G., Portnoy, D.A., and Hinrichs, D.J. (1992). Pathogenicity and immunogenicity of Listeria monocytogenes small-plaque mutants defective for intracellular growth and cell-to-cell spread. Infect. Immun. *60*, 1625–1632.

Bobay, L.M., Rocha, E.P., and Touchon, M. (2013). The adaptation of temperate bacteriophages to their host genomes. Mol. Biol. Evol. *30*, 737–751.

Bondy-Denomy, J., Qian, J., Westra, E.R., Buckling, A., Guttman, D.S., Davidson, A.R., and Maxwell, K.L. (2016). Prophages mediate defense against phage infection through diverse mechanisms. ISME J. *10*, 2854–2866.

Brüssow, H., Canchaya, C., and Hardt, W.D. (2004). Phages and the evolution of bacterial pathogens: from genomic rearrangements to lysogenic conversion. Microbiol. Mol. Biol. Rev. *68*, 560–602.

Burns, N., James, C.E., and Harrison, E. (2015). Polylysogeny magnifies competitiveness of a bacterial pathogen in vivo. Evol. Appl. *8*, 346–351.

Dorscht, J., Klumpp, J., Bielmann, R., Schmelcher, M., Born, Y., Zimmer, M., Calendar, R., and Loessner, M.J. (2009). Comparative genome analysis of Listeria bacteriophages reveals extensive mosaicism, programmed translational frameshifting, and a novel prophage insertion site. J. Bacteriol. *191*, 7206–7215.

Dubnau, D. (1999). DNA uptake in bacteria. Annu. Rev. Microbiol. *53*, 217–244.

Feiner, R., Argov, T., Rabinovich, L., Sigal, N., Borovok, I., and Herskovits, A.A. (2015). A new perspective on lysogeny: prophages as active regulatory switches of bacteria. Nat. Rev. Microbiol. *13*, 641–650.

Figueroa-Bossi, N., Uzzau, S., Maloriol, D., and Bossi, L. (2001). Variable assortment of prophages provides a transferable repertoire of pathogenic determinants in Salmonella. Mol. Microbiol. *39*, 260–271.

Hamon, M., Bierne, H., and Cossart, P. (2006). Listeria monocytogenes: a multifaceted model. Nat. Rev. Microbiol. *4*, 423–434.

Howard-Varona, C., Hargreaves, K.R., Abedon, S.T., and Sullivan, M.B. (2017). Lysogeny in nature: mechanisms, impact and ecology of temperate phages. ISME J. *11*, 1511–1520.

Johnson, A.D., Poteete, A.R., Lauer, G., Sauer, R.T., Ackers, G.K., and Ptashne, M. (1981). lambda Repressor and cro–components of an efficient molecular switch. Nature *294*, 217–223.

Klumpp, J., and Loessner, M.J. (2013). *Listeria* phages: Genomes, evolution, and application. Bacteriophage *3*, e26861.

Kulkarni, M.M. (2011). Digital multiplexed gene expression analysis using the NanoString nCounter system. Curr. Protoc. Mol. Biol. *25*, 25B.10.

Lamont, I., Brumby, A.M., and Egan, J.B. (1989). UV induction of coliphage 186: prophage induction as an SOS function. Proc. Natl. Acad. Sci. USA *86*, 5492–5496.

Lauer, P., Chow, M.Y., Loessner, M.J., Portnoy, D.A., and Calendar, R. (2002). Construction, characterization, and use of two Listeria monocytogenes site-specific phage integration vectors. J. Bacteriol. *184*, 4177–4186.

Lecuit, M. (2005). Understanding how Listeria monocytogenes targets and crosses host barriers. Clin. Microbiol. Infect. *11*, 430–436.

Little, J.W., Shepley, D.P., and Wert, D.W. (1999). Robustness of a gene regulatory circuit. EMBO J. *18*, 4299–4307.

Lwoff, A. (1953). Lysogeny. Bacteriol. Rev. *17*, 269–337.

Mandali, S., Gupta, K., Dawson, A.R., Van Duyne, G.D., and Johnson, R.C. (2017). Control of Recombination Directionality by the Listeria Phage A118 Protein Gp44 and the Coiled-Coil Motif of Its Serine Integrase. J. Bacteriol. *199*, e00019-17.

Matos, R.C., Lapaque, N., Rigottier-Gois, L., Debarbieux, L., Meylheuc, T., Gonzalez-Zorn, B., Repoila, F., Lopes, Mde.F., and Serror, P. (2013). Enterococcus faecalis prophage dynamics and contributions to pathogenic traits. PLoS Genet. *9*, e1003539.

McClure, R., Balasubramanian, D., Sun, Y., Bobrovskyy, M., Sumby, P., Genco, C.A., Vanderpool, C.K., and Tjaden, B. (2013). Computational analysis of bacterial RNA-Seq data. Nucleic Acids Res. *41*, e140.

Ohnishi, M., Kurokawa, K., and Hayashi, T. (2001). Diversification of Escherichia coli genomes: are bacteriophages the major contributors? Trends Microbiol. *9*, 481–485.

Oppenheim, A.B., Kobiler, O., Stavans, J., Court, D.L., and Adhya, S. (2005). Switches in bacteriophage lambda development. Annu. Rev. Genet. *39*, 409–429.

Osuna, B.A., Karambelkar, S., Mahendra, C., Christie, K.A., Garcia, B., Davidson, A.R., Kleinstiver, B.P., Kilcher, S., and Bondy-Denomy, J. (2019). Listeria phages induce Cas9 degradation to protect lysogenic genomes. bioRxiv. https://doi.org/10.1101/787200.

Portnoy, D.A., Jacks, P.S., and Hinrichs, D.J. (1988). Role of hemolysin for the intracellular growth of Listeria monocytogenes. J. Exp. Med. *167*, 1459–1471.

Ptashne, M. (2004). A Genetic Switch–Phage Lambda Revisited (Cold Spring Harbor Laboratory Press).

Quiles-Puchalt, N., Tormo-Más, M.A., Campoy, S., Toledo-Arana, A., Monedero, V., Lasa, I., Novick, R.P., Christie, G.E., and Penadés, J.R. (2013). A super-family of transcriptional activators regulates bacteriophage packaging and lysis in Gram-positive bacteria. Nucleic Acids Res. *41*, 7260–7275.

Rabinovich, L., Sigal, N., Borovok, I., Nir-Paz, R., and Herskovits, A.A. (2012). Prophage excision activates Listeria competence genes that promote phagosomal escape and virulence. Cell *150*, 792–802.

Rauch, B.J., Silvis, M.R., Hultquist, J.F., Waters, C.S., McGregor, M.J., Krogan, N.J., and Bondy-Denomy, J. (2017). Inhibition of CRISPR-Cas9 with Bacteriophage Proteins. Cell *168*, 150–158.e110.

Reniere, M.L., Whiteley, A.T., and Portnoy, D.A. (2016). An In Vivo Selection Identifies Listeria monocytogenes Genes Required to Sense the Intracellular Environment and Activate Virulence Factor Expression. PLoS Pathog. *12*, e1005741.

Sigal, N., Pasechnek, A., and Herskovits, A.A. (2016). RNA Purification from Intracellularly Grown Listeria monocytogenes in Macrophage Cells. J. Vis. Exp. (*112*), 54044.

Smith, K., and Youngman, P. (1992). Use of a new integrational vector to investigate compartment-specific expression of the Bacillus subtilis spoIIM gene. Biochimie *74*, 705–711.

Stead, M.B., Agrawal, A., Bowden, K.E., Nasir, R., Mohanty, B.K., Meagher, R.B., and Kushner, S.R. (2012). RNAsnap™: a rapid, quantitative and inexpensive, method for isolating total RNA from bacteria. Nucleic Acids Res. *40*, e156.

Swaminathan, B., and Gerner-Smidt, P. (2007). The epidemiology of human listeriosis. Microbes Infect. *9*, 1236–1243.

Tjaden, B. (2015). De novo assembly of bacterial transcriptomes from RNA-seq data. Genome Biol. *16*, 1.

Toledo-Arana, A., Dussurget, O., Nikitas, G., Sesto, N., Guet-Revillet, H., Balestrino, D., Loh, E., Gripenland, J., Tiensuu, T., Vaitkevicius, K., et al. (2009). The Listeria transcriptional landscape from saprophytism to virulence. Nature *459*, 950–956.

Waldor, M.K., and Friedman, D.I. (2005). Phage regulatory circuits and virulence gene expression. Curr. Opin. Microbiol. *8*, 459–465.

Wang, X., Kim, Y., Ma, Q., Hong, S.H., Pokusaeva, K., Sturino, J.M., and Wood, T.K. (2010). Cryptic prophages help bacteria cope with adverse environments. Nat. Commun. *1*, 147.

Zink, R., and Loessner, M.J. (1992). Classification of virulent and temperate bacteriophages of Listeria spp. on the basis of morphology and protein analysis. Appl. Environ. Microbiol. *58*, 296–302.

STAR★METHODS

KEY RESOURCES TABLE

REAGENT or RESOURCE	SOURCE	IDENTIFIER
Antibodies		
anti-6His tag antibody	Abcam	ab18184; RRID: AB_444306
anti-listeria-FITC antibody	Bio-Rad	0400-0027; RRID: AB_619120
Bacterial and Virus Strains		
Lm 10403S	Prof. Daniel Portnoy (University of California, Berkley)	N/A
Chemicals, Peptides, and Recombinant Proteins		
mitomycin C	Sigma	M4287
rhodamine-phalloidin	Biotium	#00027
Brain Heart Infusion Broth	Sigma	53286-500G
Critical Commercial Assays		
Ribo-Zero rRNA Removal Kit (Bacteria)	Illumina	MRZB12424
RNAeasy kit	QIAGEN	74104
NEBNext® Ultra Directional RNA Library Prep Kit for Illumina	NEB	E7420S
Deposited Data		
RNA-Seq data (BHI)	This study	Mendeley Data: https://doi.org/10.17632/kjyh2swhg9.1
RNA-Seq data (UV treated)	This study	Mendeley Data: https://doi.org/10.17632/mz484h884h.2
Source file including raw experimental data	This study	Mendeley Data: https://doi.org/10.17632/9jzf6vk3p7.1
Experimental Models: Organisms/Strains		
C57BL/6JOlaHsd mice, 8-week old	Envigo, Israel	N/A
Oligonucleotides		
See Table S4	This study	N/A
Recombinant DNA		
*pheS**	Argov et al., 2017b	Addgene, 98783
Software and Algorithms		
StepOne V2.1	Applied Biosystems	N/A
nSolver 4.0 software	Kulkarni, 2011	N/A
Other		
nCounter system	NanoString Technologies	N/A
Synergy HT	BioTek	N/A

RESOURCE AVAILABILITY

Lead Contact

Further information and requests for resources and reagents should be directed to and will be fulfilled by the Lead Contact, Anat A. Herskovits (anathe@tauex.tau.ac.il).

Materials Availability

This study did not generate new unique reagents. The plasmids and strains used in this study will be made available on request, but we may require a payment and/or a completed Materials Transfer Agreement if there is potential for commercial application.

Data and Code Availability

The RNA-Seq data are available in Mendeley Data via these links:

Mendeley Data: https://doi.org/10.17632/kjyh2swhg9.2

Mendeley Data: https://doi.org/10.17632/mz484h884h.3

Source file including raw experimental data

Mendeley Data: https://doi.org/10.17632/9jzf6vk3p7.1

EXPERIMENTAL MODEL AND SUBJECT DETAILS

Bacterial strains

Listeria monocytogenes (*Lm*) strain 10403S was obtained from Prof. Daniel Portnoy (University of California, Berkley) and used as the WT strain. *Lm* 10403S strain cured of ϕ10403S phage (DPL-4056) was generated by Prof. Richard Calendar (University of California, Berkley) by biological curing. *E. coli* XL-1 Blue (Stratagene) was utilized for vector propagation. *E. coli* SM-10 was utilized for conjugative plasmid delivery to *Lm* bacteria. *Lm* strains were grown in brain heart infusion (BHI) (Merck) medium at 37°C or 30°C as specified, and *E. coli* strains were grown in Luria-Bertani (LB) (Acumedia) medium at 37°C. *B. subtilis* strain PY79 was obtained from Prof. Avigdor Eldar (Tel Aviv University). The strains and mutants used in this study are described further in Table S6.

Animals

The use of animals in this study was approved by the Tel Aviv University Animal Care and Use Committee (04-18-028 and 04-20-005) according to the Israel Welfare Law (1994) and the National Research Council guide (Guide for the Care and Use of Laboratory Animals 2010). Animals used were 8-week-old female C57BL/6 mice (Envigo, Israel). Mice were infected via the tail vein or used for bone marrow derived macrophages (BMDM) isolation. BMDMs were cultured in Dulbecco's Modified Eagle Medium (DMEM)-based media supplemented with 20% fetal bovine serum, sodium pyruvate (1 mM), L-glutamine (2 mM), β- Mercaptoethanol (0.05 mM), and monocyte-colony stimulating factor (M-CSF, L929-conditioned medium); BMDM medium.

METHOD DETAILS

Generation of gene deletion mutants and overexpression strains

All in-frame deletions generated in this work were constructed using the *Lm* 10403S strain as the parental strain. Upstream and downstream regions of selected genes were amplified using Phusion DNA polymerase and cloned into pKSV7oriT vector (Smith and Youngman, 1992). Cloned plasmids were sequenced and conjugated to *Lm* using the *E. coli* SM-10 strain. *Lm* conjugants were then grown at 41°C for two days in BHI with chloramphenicol to promote plasmid integration into the bacterial chromosome by homologous recombination. For plasmid curing, bacteria were passed several times in fresh BHI without chloramphenicol at 30°C to allow plasmid excision via the generation of an in-frame deletion. The bacteria were then seeded on BHI plates and chloramphenicol sensitive colonies were picked for validation of gene deletion using PCR. The *llgA* expressing strains were generated by using the pPL2 integrative plasmid to introduce a copy of the *llgA* gene in *trans* under the control of P*actA* or P*tetR* promoters (Lauer et al., 2002). For the detection of LlgA activity under 30°C and 37°C, a reporter system was designed that includes the *llgA* gene under the regulation of a TetR dependent promoter, cloned up-stream to *terS* gene with its upstream region, including LlgA putative binding sites (according to Quiles-Puchalt et al., 2013). For the expression of this system in *B. subtilis* strain PY79, the *llgA-terS* cassette was cloned in the AES777 plasmid under the inducible hyperspank (*hs*) promoter. The construct was then introduced into *B. subtilis* chromosome, in the *amyE* gene, using standard transformation and Spp1 transduction protocols (*amyE*::P*hs-llgA-terS*) (Bareia et al., 2018).

Phage induction by UV irradiation

Lm bacteria were grown in BHI medium over-night (O.N.) at 37°C with agitation. To obtain lysogenic bacteria, the culture was diluted by a factor of 100 in fresh BHI and incubated without agitation at 30°C to reach OD_{600} of 0.7-0.8. For induction of the lytic cycle, O.N. cultures were diluted by a factor of 10 in 10 mL of fresh BHI, and incubated without agitation at 30°C to reach an OD_{600} of 0.5. The cultures were then irradiated by UV light at 4 J/cm^2 (using CL 508S model UV cross-linker oven), were supplemented with 5 mL of fresh BHI medium, and were then incubated without agitation at 30°C. At specified time points, the cultures were either filtered through 0.22 μm filters to isolate virions, or centrifuged to collect bacteria that were snap-frozen in liquid nitrogen for further transcription analysis.

One-step phage growth analysis and plaque assay

For the one-step growth analysis over-night cultures of *Lm ΔcomK* bacteria were diluted in 10 mL of BHI to an OD_{600} of 0.1, and incubated with agitation at 30°C to reach an OD_{600} of 0.5 (~5*10^8 cells/ml). The cultures were then supplemented with 10 mM $CaCl_2$ and infected with 0.5 mL of isolated virions (10^8 virions/ml, induced by MC) at a multiplicity of infection of ~100:1 (bacteria:virions) for 10 min at 30°C (the adsorption step). One ml of culture was then centrifuged at 16000 g for 1 min and resuspended in fresh BHI to remove unattached virions. A 0.1 mL aliquot of the sample was then diluted into 10 mL of fresh pre-warmed BHI (to avoid a second infection) and incubated at 30°C without shaking. Samples were collected every 20 min, and plaque forming units (PFUs)

were quantified by adding 100 μL of virion containing sample at appropriate dilution, to 300 μL of an O.N. culture of *Lm* Mack861 bacteria (used as the indicator strain). Three ml of melted LB-0.7% agar medium (at 56°C) supplemented with 10 mM $CaCl_2$, was added, mixed, and then quickly overlaid on BHI-agar plates. Plates were incubated for 2 days at 30°C to allow the formation of visible plaques. To calculate the phage burst size the PFU number at the plateau (~1000) was divided by the PFU number at the latent period (~25), yielding ~40 virions per infected cell.

Transmission electron microscopy

4 h post UV irradiation, bacteria were collected by centrifugation and fixed in 2.5% glutaraldehyde in PBS over night at 4°C. After several washings in PBS, the bacteria were post fixed in 1% OsO_4 in PBS for 2 h at 4°C. Dehydration was carried out in graded ethanol followed by embedding in glycidether. Thin sections were mounted on Formvar/Carbon coated grids, stained with uranyl acetate and lead citrate, and examined by a Jeol 1400 – Plus transmission electron microscope (Jeol, Japan). Images were captured using SIS Megaview III and iTEM the TEM imaging platform (Olympus).

RNA-seq analysis

Analysis of the phage transcription profile under lysogenic and lytic conditions was performed using strand-specific RNA-seq analysis by Illumina. Bacteria were grown in BHI medium (with and without UV irradiation) and harvested at 4 h post UV irradiation for RNA-seq analysis. Total bacterial RNA was extracted using the RNAsnap method (Stead et al., 2012) followed by DNase I (QIAGEN) treatment on QIAGEN RNAeasy columns. The RNA integrity number (RIN) was evaluated using a TapeStation instrument (Agilent Technologies) (the RIN values ranged from 7.5 to 9.6, except for one sample that was 7.1), and then the rRNA was depleted using the Ribo- Zero kit (Illumina). Strand specific RNA-seq libraries were prepared using the NEBNext® Ultra Directional RNA Library Prep Kit for Illumina (NEB) and sequenced (50 nt per read) by HiSeq 2500 instrument (Illumina) at the Technion Genome Centre (Haifa, Israel). Mapping of reads followed by upper quartile normalization by gene expression and differential expression analysis by the negative binomial distribution as the statistical model was performed using Rockhopper V2.03 with default parameters (McClure et al., 2013; Tjaden, 2015). The complete results are provided in Table S3. The heatmap was generated using R plotting. The RNA-seq analysis was performed on three independent biological repeats.

NanoString analysis of phage transcripts in intracellularly grown bacteria

To analyze the transcription profile of ϕ10403S during *Lm* infection of macrophages the NanoString technology was employed (using the nCounter system), which is based on the hybridization of specific fluorescently labeled probes (Kulkarni, 2011). Sixty phage-specific barcoded probes were designed (~80-100 nucleotides each) that, based on the Illumina sequencing data, cover all the phage transcripts from both strands. RNA was purified from intracellularly grown bacteria in bone marrow-derived macrophage cells (BMDM) at time points 2, 4 and 6 h post infection as described previously (Sigal et al., 2016). BMDM cells used for infection experiments were isolated from 6–8 week-old female C57BL/6 mice (Envigo, Israel) as described previously (Portnoy et al., 1988) and cultured in Dulbecco's Modified Eagle Medium (DMEM)-based media supplemented with 20% fetal bovine serum, sodium pyruvate (1 mM), L-glutamine (2 mM), β- Mercaptoethanol (0.05 mM), and monocyte-colony stimulating factor (M-CSF, L929-conditioned medium); BMDM medium. For each time point, three 145 mm dishes were seeded with 2×10^7 BMDMs that were then infected (in parallel) with 2×10^9 of WT *Lm* bacteria. 30 min post infection, BMDM monolayers were washed twice with PBS to remove unattached bacteria, and fresh medium was added. At 1 h post-infection (h.p.i.), gentamicin (50 μg/ml) was added to limit extracellular bacterial growth. At 2, 4, and 6 h. p. i. the macrophages were lysed with 20 mL cold water, and cell debris and nuclei were removed by centrifugation at 800 g for 3 min at 4°C. Released bacteria were quickly collected on 0.45 μm filter membranes (Millipore) using a vacuum apparatus and snap-frozen in liquid nitrogen. Bacteria were recovered from the filters by vortexing into AE buffer (50 mM sodium acetate pH 5.2, 10 mM EDTA), and bacterial nucleic acids were extracted using RNAsnap followed by ethanol precipitation (Stead et al., 2012). RNeasy Mini Kit DNase on column (QIAGEN) was used for DNase treatment. For nCounter analysis of mRNA transcripts, a multiplexed CodeSet was assembled with two sequence-specific probes for each target gene of interest (Table S4). A 150 ng aliquot of each RNA sample was hybridized with the CodeSet. Transcription levels of phage genes in total RNA samples were measured with specific probes using the NanoString nCounter system, according to the manufacturer's standard procedures. Images of color-coded reporter probes bound to their complementary mRNA target, image acquisition, and data processing were collected in a reporter code count (RCC) file and the raw counts were normalized to the internal positive controls; *rpoD*, *bglA,* and *rpoB* using the nSolver 4.0 software (Kulkarni, 2011). The data were normalized to the counts detected in samples of lysogenic WT *Lm* bacteria and are presented as a relative quantity (RQ). The complete results are provided in Table S5. The heatmap was generated with R plotting. The NanoString analysis was performed on three independent biological repeats.

Lm intracellular growth

In order to assess the intracellular growth of *Lm* bacteria, 2×10^6 BMDM cells were seeded in a 60 mm Petri dish on glass coverslips in 5 mL of BMDM medium and incubated O.N. in a 37°C, 5% CO_2 forced-air incubator. *Lm* bacteria were grown O.N. at 30°C without agitation and 8×10^6 bacteria were used to infect BMDM cells. 30 min post-infection, the macrophage monolayers were washed and fresh medium was added. Gentamicin was supplemented at 1 h.p.i. (50 μg/ml) to limit the growth of extracellular bacteria. At the indicated time points, three coverslips were transferred into 2 mL of sterile water and vortexed to release intracellular bacteria.

Appropriate dilutions of the resulting lysate were plated on BHI agar plates and CFUs were counted after 24 h of incubation at 37°C. Each experiment was repeated at least three times.

Phagosomal escape assay

1×10^6 BMDM cells were seeded on 20 mm coverslips and infected as described above. Cells were fixed at 2.5 h.p.i. with 3.7% paraformaldehyde, and permeabilized with 0.05% Triton. Slides were then washed and stained appropriately: bacteria were stained with anti-listeria-FITC antibody (Bio-Rad); actin was stained with rhodamine-phalloidin (Biotium); and DNA was stained with DAPI containing Vectashield® mounting media. Images were collected using a Nikon eclipse Ti-E microscope. For each infection experiment ~200 bacteria were counted in 4-5 different frames and statistical analysis was performed using χ-test.

Phage loss assays

To measure the loss of ϕ10403S-prophage from the *Lm* chromosome, *pheS** (encoding a mutated phenylalanyl-tRNA synthetase) (Argov et al., 2017b) and kanamycin resistance genes were cloned into the phage genome downstream to the *LMRG_01556* gene in WT *Lm* and Δ*LMRG_01526* bacteria. These strains were then used to infect macrophage cells for 6 h as described above (Intracellular growth of *Lm*). For *in vivo* experiments, 8-week-old female C57BL/6 mice (Envigo, Israel) were infected via the tail vein with 1.5×10^5 bacteria in 200 μl PBS. Animals were observed daily for any signs of illnesses and were euthanized at 48 h.p.i. Spleens and livers were harvested and homogenized in 0.2% saponin. Bacteria were released from BMDMs or organs and plated on BHI-agar plates to quantify total CFU, and on selective *p*-chloro-phenylalanine (18 mM) plates for phage-cured bacteria (Argov et al., 2017b). Phage-loss in bacteria growing on *p*-Cl^-phe plates was verified by re-plating on kanamycin-selective plates and by PCR.

qRT-PCR analysis

Total nucleic acids were isolated from bacterial pellets through standard phenol-chloroform extraction methods. An aliquot of 0.04 ng of total nucleic acids was used for qRT-PCR analysis of *attB* and *attP* levels with bacterial 16S rRNA gene used as a reference for sample normalization. For transcription analysis, samples were treated with DNaseI, and 1 μg of RNA was reverse transcribed to cDNA using a qScript (Quanta) kit. qRT-qPCR was performed on 10 ng of cDNA. The relative transcription of bacterial genes was determined by comparing the level of transcript with bacterial 16S rRNA or *rpoD* genes, which served as a reference. All qRT-qPCR analyses were performed using FastStart Universal SYBR Green Master Mix (Roche) on the StepOnePlus RT-PCR system (Applied Biosystems). Statistical analysis was performed using StepOne V2.1 software. Error bars represent the 95% confidence interval.

Growth of LlgA expressing bacteria

Single colonies of *Lm* strains (WT, $\Delta(lysis)_\phi$, and $\Delta\phi$) harboring a C'-His-tagged *llgA* gene under the regulation of a TetR dependent promoter on the integrative pPL2 plasmid (pPL2-P*tetR-llgA-his*) were suspended in BHI medium with or without the TetR inducer anhydrotetracycline (AT, 10 ng/ml) and 200 μl were pipetted in triplicates into a 96-well plate. Plates were incubated at 30°C or 37°C using a Synergy HT BioTek plate reader, and OD_{600} measurements were taken every 15 min, preceding 1 min of shaking. For transcription analysis, *Lm* bacteria were grown in BHI and *B. subtilis* bacteria were grown in Luria-Bertani (LB) medium with the addition of 10 μM IPTG, at 30°C and 37°C. The bacteria were collected by centrifugation at exponential phase and snap-frozen in liquid nitrogen for further transcription analysis.

Western blot analysis

Lm $\Delta(lysis)_\phi$ and $\Delta\phi$ strains harboring 6His-tagged *llgA* under the regulation of a TetR dependent promoter in the integrative pPL2 plasmid (pPL2-P*tetR-llgA-his*) were grown at 30°C or 37°C in 50 mL BHI to an OD_{600} of 0.6. The bacteria were then collected by centrifugation and washed with Buffer-A (20mM Tris-HCl pH 8, 0.5M NaCl, and 1 mM EDTA), suspended in 1 mL Buffer-A supplemented with 1 mM PMSF and lysed by ultra-sonication. Total protein content was assayed using a modified Lowry assay and samples with equal amounts of total proteins were separated on 15% SDS-polyacrylamide gels and transferred to nitrocellulose membranes. Proteins were probed with mouse anti-6His tag antibody (Abcam ab18184) at 1:1000 dilution, followed by HRP-conjugated goat anti-mouse IgG (Jackson ImmunoResearch, USA) at 1:20,000 dilution. Western blots were developed by a homemade enhanced chemiluminescence reaction (ECL).

QUANTIFICATION AND STATISTICAL ANALYSIS

All data are presented as mean of three biological repeats (n = 3) ± 1 standard deviation, unless indicated otherwise. Statistical significance was calculated using Student's t test, except for Figure 4B where it was calculated by the χ-test. Replicate values in Figures 4C, 5, and 6A are in triplicates. For each intracellular growth experiment and western blotting analysis a representative experiment is shown, and additional biological repeats can be found in the provided raw data file. For qRT-PCR experiments statistical analysis was performed using StepOne V2.1 software and error bars represent the 95% confidence interval. Details of statistical analysis can be found in the Figure Legends.

Cell Reports, Volume *32*

Supplemental Information

Active Lysogeny in *Listeria Monocytogenes* Is a Bacteria-Phage Adaptive Response in the Mammalian Environment

Anna Pasechnek, Lev Rabinovich, Olga Stadnyuk, Gil Azulay, Jessica Mioduser, Tal Argov, Ilya Borovok, Nadejda Sigal, and Anat A. Herskovits

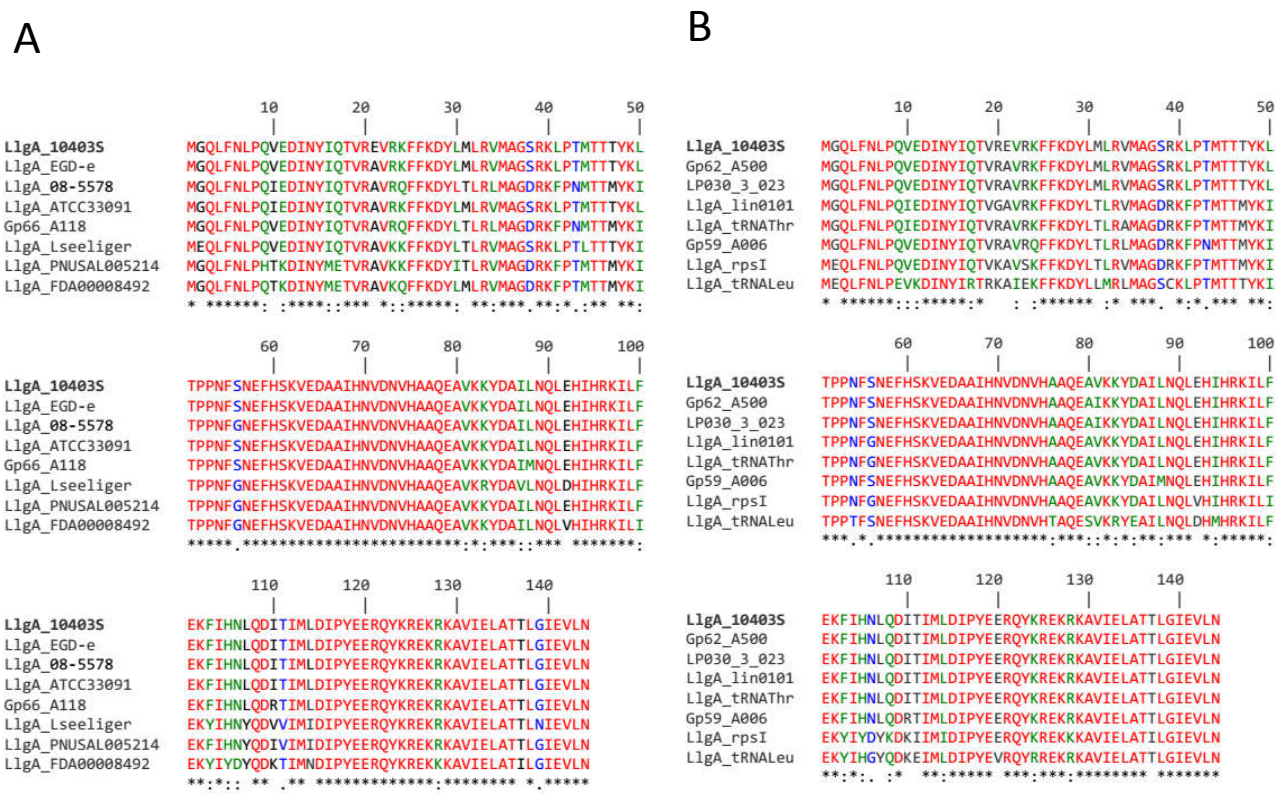

Figure S1. Comparison of ϕ10403S LlgA orthologs. Related to Figure 6. **A.** Comparison of ϕ10403S LlgA orthologs encoded by selected *comK* associated prophages of *Listeria*. Alignment length: 144 residues. Identical residues (marked with asterisks and shown in red) are 75.69 % (109/144), strongly similar residues (marked with colons and shown in green) are 13.89 % (20/144), weakly similar (marked with dots and shown in blue) are 3.47 % (5/144), and different are 6.94 % (10/144). LlgA_10403S (LMRG_01529, 144 aa), *comK* associated prophage ϕ10403S, *L. monocytogenes* str. 10403S. LlgA_EGD-e (lmo2303, 144 aa), *comK* associated prophage, *L. monocytogenes* str. EGD-e. LlgA_08-5578 (LM5578_2501, 144 aa), *comK* associated prophage, *L. monocytogenes* str. 08-5578. LlgA_ATCC33091 (EHN62215.1, 144 aa), *comK* associated prophage, *L. innocua* str. ATCC 33091. Gp66_A118 (Gp66, NP_463531.1, 144 aa), *comK* associated *Listeria* phage A118. LlgA_Lseeliger (OLQ23568.1, 144 aa), *comK* associated prophage, *L. seeligeri* str. BCW_4759. LlgA_PNUSAL005214 (ECK6838613.1, 144 aa), *comK* associated prophage, *L. monocytogenes* str. PNUSAL005214. LlgA_FDA00008492 (EAC8843104.1, 144 aa), *L. monocytogenes* str. FDA00008492. **B.** Comparison of ϕ10403S LlgA orthologs encoded by selected non-*comK* associated prophages of *Listeria*. Alignment length: 144 residues. Identical residues (marked with asterisks and shown in red) are 70.14 % (101/144), strongly similar residues (marked with colons and shown in green) are 15.97 % (23/144), weakly similar (marked with dots and shown in blue) are 3.47 % (5/144), and different are 10.42 % (15/144). LlgA_10403S (144 aa, LMRG_01529), *comK* gene prophage ϕ10403S, *L. monocytogenes* str. 10403S. Gp62_A500 (144 aa, Gp62, YP_001468447.1), tRNA-Lys gene *Listeria* phage A500. LP030_3_023 (144 aa, YP_009044669.1), tRNA-Lys gene *Listeria* phage LP-030-3. LlgA_lin0101 (144 aa, lin0101), tRNA-Lys gene prophage, *L. innocua* str. Clip11262. LlgA_tRNAThr (144 aa, LMOSLCC7179_2533), tRNA-Thr gene prophage, *L. monocytogenes* SLCC 7179 (serotype 3a). Gp59_A006 1 (144 aa, Gp59, YP_001468899.1), tRNA-Arg gene *Listeria* phage A006. LlgA_rpsI (144 aa, EAV9834825.1), *rpsI* gene prophage, *L. monocytogenes* L7-0863. LlgA_tRNALeu (144 aa, EAC7181297.1), tRNA-Leu prophage, *L. monocytogenes* PNUSAL001712 (serotype 4b).

Table S1. Lytic induction of ϕ10403S and ϕEGDe *comK*-prophages by mitomycin C. Related to Figure 1.

Strain/treatment	PFU/ml	STD
Lm 10403S -MC	108,500	48,000
Lm 10403S +MC	444,500,000	55,700,00
Lm EGDe -MC	0	0
Lm EGDe +MC	15	21

Table S2: A list of ϕ10403S genes and annotations. Related to Figure 2A.

Gene	Strand	Annotation/Putative function	Detected transcripts (by RNA-seq)	Ortholog in A118
LMRG_01560	+	N-terminus of competence regulator ComK		
LMRG_01559	-	Conserved hypothetical protein	+	-
LMRG_01558	-	Conserved hypothetical protein	+	-
rli43-like*	-	Ortholog of Rli43 of *Lm* EGDe	-	-
LMRG_01557	-	Putative secreted protein	-	-
rli34-like*	+	Rli34 ortholog of *Lm* EGDe	-	-
LMRG_01556	-	Putative acetyltransferase	+	gp27
LMRG_01555	-	Conserved hypothetical protein	+	gp26
LMRG_01554	-	Endolysin	+	gp25
LMRG_01553	-	Holin	+	gp24
LMRG_01552	-	Membrane-associated protein	+	gp23
LMRG_01551	-	Conserved hypothetical protein	+	gp22
LMRG_01550	-	Hypothetical protein	+	gp21
LMRG_01549	-	Secreted receptor-binding protein (RBP)	+	gp20
LMRG_01548	-	Secreted pectin-lyase-fold protein	+	gp19
LMRG_01547	-	Tail or base plate protein with a putative endopeptidase activity	+	gp18
LMRG_01546	-	Tail protein	+	gp17
LMRG_01545	-	Tape-measure protein	+	gp16
LMRG_01544	-	Conserved hypothetical protein	+	gp15
LMRG_01543	-	Tail assembly chaperone protein	+	gp14
LMRG_01542	-	Cell surface and adhesion associated protein	+	gp13
LMRG_01541	-	Conserved hypothetical protein	+	gp12
LMRG_01540	-	Minor capsid protein	+	gp11
LMRG_01539	-	Minor capsid protein	+	gp10
LMRG_01538	-	Minor capsid protein	+	gp9
LMRG_01537	-	Head-tail connector protein YqbG	+	gp8
LMRG_01536	-	Capsid protein	+	-
LMRG_01535	-	Minor structural protein of GP20-family, scaffolding protein	+	gp5
LMRG_01534	-	Minor capsid protein	+	gp4
LMRG_01533	-	Portal protein	+	gp3
LMRG_01532	-	Terminase large subunit, TerL, XtmB family	+	gp2
LMRG_01531	-	Terminase small subunit, TerS, XtmA family	+	gp1
LMRG_01530	-	Membrane-associated protein	+	gp68
rliG-like*	-	RliG ortholog of *Lm* EGDe	+	*
LMRG_01529	-	Late lytic genes activator, LlgA, transcriptional regulatory protein of the ArpU family	+	gp66
LMRG_01528	-	Conserved hypothetical protein	+	gp65
LMRG_02921	-	Conserved hypothetical protein	+	-
LMRG_01527	-	Conserved hypothetical protein	+	-
LMRG_01526	-	DnaD-like DNA replication protein, replicase	+	gp49
LMRG_01525	-	Recombinational DNA repair protein RecT, recombinase	+	gp48
LMRG_01524	-	Predicted endonuclease	+	gp47
rli99-like*	+	Rli99 ortholog of *Lm* EGDe	-	-
rli140-like*	-	Rli140 ortholog of *Lm* EGDe	+	-
gp46-like*	-	Hypothetical protein	-	gp46
LMRG_01510	+	C-terminus of competence regulator ComK		

Table S2: continued

LMRG_01523	-	Conserved tail-fibre system protein	+	gp45
LMRG_01522	-	Recombination Directionality Factor (RDF)	+	gp44
LMRG_01521	-	Conserved hypothetical protein	+	gp43
LMRG_02920	-	Putative anti-repressor protein	+	gp42
lasRNA-like*	+	Long anti-sense RNA of LMRG_01516-01517-01518-02984 as identified in EGDe *comK*-prophage. Includes a putative ORF similar to gp41-1 of A118	+	-
LMRG_02984	-	Putative membrane-associated protein	+	*
LMRG_01518	-	Hypothetical protein	+	gp41
LMRG_01517	-	Conserved hypothetical protein	+	-
LMRG_01516	-	Conserved hypothetical protein	+	-
LMRG_01515	-	Cro-like transcriptional regulator, XRE-family protein	+	gp36-1**
LMRG_01514	+	CI-like transcriptional regulator, XRE-family protein	+	gp36**
rli141-like*	+	Rli141 ortholog of *Lm* EGDe	-	-
LMRG_02918	+	Conserved hypothetical protein	+	-
LMRG_01513	+	Putative secreted Lpt-like lipoprotein	+	gp32
LMRG_01512	+	Putative DNA helicase	+	-
LMRG_01511	+	Site-specific phage serine integrase	+	gp31

*** present but not annotated**
**** low similarity**

Table S3. ϕ10403S transcriptional response under lysogenic and lytic conditions. Related to Figure 2B-C.

Transcription Start	Translation Start	Translation Stop	Transcription Stop	Strand	Genes	Time post UV irradiation					
						0h	**1h**	**2h**	**3h**	**4h**	**5h**
	2357429	2357878		+	comk C'	7	7	9	5	4	1
	2356053	2357411	2357411	+	LMRG_01511	58	40	40	49	50	24
2354478	2354478	2355992	2355992	+	LMRG_01512	29	33	26	27	31	15
2353710	2353710	2354246		+	LMRG_01513	41	77	59	31	31	21
2353494	2353494	2353661		+	LMRG_02918	24	55	38	24	24	16
2352860	2352860	2353336	2353336	+	LMRG_01514	79	134	102	34	31	20
2352691	2352691	2352488	2352488	-	LMRG_01515	14	32	109	195	312	226
2352487	2352455	2352261	2352250	-	LMRG_01516	16	37	120	268	427	318
2352249	2352249	2351965	2351947	-	LMRG_01517	19	50	149	336	520	397
2351946	2351939	2351658	2351653	-	LMRG_01518	15	43	130	302	450	371
2351632			2351664	+	lasRNA	388	83	125	283	371	452
2351652	2351652	2351377		-	LMRG_02984	17	52	161	351	579	438
	2351395	2350616	2350576	-	LMRG_02920	25	53	176	379	554	425
2350510	2350494	2349961		-	LMRG_01521	15	35	121	229	333	259
	2349964	2349749	2349743	-	LMRG_01522	9	16	66	151	253	197
2349647	2349640	2349452	2349446	-	LMRG_01523	9	17	74	176	276	201
2349421			2349324	-	rli140	21	37	155	320	485	368
2349221	2349219	2348260		-	LMRG_01524	14	31	124	280	402	324
	2348260	2347445	2347426	-	LMRG_01525	23	56	206	437	620	485
2347425	2347425	2346499		-	LMRG_01526	21	46	163	359	509	389
	2346502	2346251	2346251	-	LMRG_01527	16	39	144	295	426	344
2346250	2346248	2345724	2345704	-	LMRG_02921	14	43	137	286	434	331

Table S3 continued

2345686	2345676	2345512	2345512	-	LMRG_01528	13	35	106	244	375	297
2345511	2345493	2345059	2345000	-	LMRG_01529	15	41	146	278	412	304
2344909			2344775	-	rliG	126	496	1366	1943	1944	1327
2344696	2344692	2343982	2343982	-	LMRG_01530	14	32	78	215	332	190
2343898	2343898	2343356		-	LMRG_01531	11	23	74	184	321	181
	2343387	2342056	2342044	-	LMRG_01532	8	19	55	150	263	145
2342043	2342043	2340553	2340553	-	LMRG_01533	14	32	100	251	443	257
2340552	2340547	2339408	2339408	-	LMRG_01534	16	38	115	296	503	293
2339388	2339329	2338739		-	LMRG_01535	31	79	256	757	1343	807
	2338739	2337738	2337738	-	LMRG_01536	29	73	238	733	1261	754
2337737	2337719	2337324		-	LMRG_01537	23	70	211	710	1235	755
	2337324	2336962		-	LMRG_01538	22	67	211	667	1161	717
	2336962	2336624		-	LMRG_01539	31	89	272	860	1490	914
	2336624	2336217	2336215	-	LMRG_01540	22	59	186	648	1085	695
2336214	2336214	2335777	2335777	-	LMRG_01541	25	69	223	672	1132	729
2335776	2335754	2335515	2335515	-	LMRG_01542	28	83	255	808	1370	876
2335514	2335460	2335038	2335038	-	LMRG_01543	14	31	117	381	700	371
2335034	2335032	2334430	2334425	-	LMRG_01544	12	30	100	317	591	309
2334419	2334419	2329056	2329056	-	LMRG_01545	10	22	73	220	430	243
2329055	2329054	2328236	2328228	-	LMRG_01546	8	24	66	201	403	294
2328227	2328227	2327202		-	LMRG_01547	8	23	63	204	396	272
	2327201	2326173		-	LMRG_01548	7	20	54	168	334	242
	2326173	2325100	2325100	-	LMRG_01549	6	19	48	140	288	214
2325093	2325088	2324771	2324771	-	LMRG_01550	4	13	38	124	276	199
2324770	2324766	2324608	2324590	-	LMRG_01551	6	16	51	163	357	262
2324579	2324579	2324214	2324214	-	LMRG_01552	3	11	33	109	241	197
2324213	2324201	2323920		-	LMRG_01553	3	12	35	104	230	187

Table S3 continued

	2323920	2323069	2323069	-	LMRG_01554	5	20	54	172	343	301
2322830	2322830	2322654		-	LMRG_01555	300	273	249	197	333	241
	2322667	2322068	2322068	-	LMRG_01556	184	185	150	119	187	160
	2321545	2320622		-	LMRG_01557	2	2	2	2	3	0
2320365	2320365	2320132		-	LMRG_01558	29	318	295	194	261	211
	2320135	2319938	2319937	-	LMRG_01559	47	400	360	298	370	330
	2319659	2319937	2319937	+	comK N'	7	16	10	7	5	4

Table S4: A list of ϕ10403S nCounter probes. Related to Figure 3.

Gene	Probe sequence
	TACGTCTGCTACGTAGAAGGAAAAGATAAAGCTATAGAAAAGCTGTTTGCCGAATTAT
LMRG_01559	TTGAAACAAGAAAGTTAAAGACCTTACAAAGGCGTATAAAAA
	ATAGTATTAGCAGACGCGCTTAGGCGCAATTGGTCAATAGAAGTACTGTTTTTAAAGA
LMRG_01558	ACAATCATCACGTGCGATACAAGTATGTCGTGCCTGTCCACA
	TGGTTTAACTATGCGTTATACTTCAAAGGCAGGAACTTGGGATACTTCGGCATGGAAAG
LMRG_01557	TAGTTTCCGCCAGTACTAAAACGACAGATAAATATGCGCAG
	GGAGTAATCGAGTTTACAAGAAGAAACGATAAATTTGTCCGGCATACACCGGGTTTTG
LMRG_01556	ATAGTAATACTATGTTTGCTGATGGAGGGAATCAAACCTATC
	TTTCGGAAAGAAAAGCAATTGCTAGTATAAGAGAGAATTTTGCACAAATTCCAAAGAT
LMRG_01555	GAACATTACTAATGACAAGAGATAA
	TTGGGGCGCTTATCGTTCAGATAAAGGCAAGAAATTTGTGGCAAAAGCGAAGGCACTT
LMRG_01554	GGATTTGAATGGGGCGGTGATTGGTCTGGATTTGTAGACAAT
	GTGGCTTCCGACTGTTAGCATACTTATTGGTGCTATTCTGGGCGCATTAGCAACGTTTTT
LMRG_01553	GGATGGCTCTGGATCGCTTGCAACGATGATTTGGGCAGGT
	TATAAGTACGATGAACGAACAACAGCGATTGATGGATAGGCAAAATGACATGATGAA
LMRG_01552	ACAGCAACAACAATCAATTGACAGCTTGTCTAAATCAGTCGGA
	ATTGAAGAAGTTCCTGCGAATTTACGAGGTCAGGTAAAAGCAAAAGTGGATGAGTTAA
LMRG_01551	AACAAGAACAACAACGAATACAGTCAGAAGAAATAGAAGCCG
	ACCTTCCATAATAGAAAACGGCATAGCAAGAGCAATGTATTATCCGCGTTGGGATGGG
LMRG_01550	GATGATTGGGACGAAGACAAGACGAGATGGGAATTAGAAAAC
	AACACAAGCATTCATGTGACAATGACTGATAAAACGAATTGGAATGCAAAAGAAAATA
LMRG_01549	CCGCGGGATCGCAAGCAAAAGCGGATAGTGCATTAAACTCTG
	AACTTCGAATGTCGGCTTAAAAGCTGCTAGCGGAGGCATTTTGGTTAAGTCTGGTACGC
LMRG_01548	CAGTTTTAAACGCTACTACCGCAGAATTGAAACAAGCGGGA
	ACACTGTTGCAGGTAATATGCAACGGCGTCTTAAGCTAGAATTACAAGACTATCCAGC
LMRG_01547	GACGACAGGAAGTGTGACCTTAAAACAATACTACGATTGTGG
	CATTCTAAAACGCCTGGTAAAAAATATAGAGTACATCCGAGTGGCGTTGGTATTGACC
LMRG_01546	GCAAAGCGCCGGGATACGCAGATTTGACACTTGAATTCGATG
	ACAGCAGTGATAGGGTCTGTAGTGGCAGTTCTTTATGGCATGTATACCGCCTTCAAGGA
LMRG_01545	AAACACGGCAGGGATTAAAGGCTTTTTATCTGGTATGTGGG
	GATGGTTTGCTTTATGATATCGACGGAAACAAGATGCCAAGCGCTACAAACAATGAGG
LMRG_01544	ATGCGGAAGAAATTGCTTCATATTCATTAACGCAAGATGCGG
	ACTGGACAAATTGGATAAATACAACTTAGACGAATTAGGCGAAATGACTATAAATGAT
LMRG_01543	TACGATGTCTTAATGGACAATGTCAGAGAGGCGCTCAAACAC
	GTAACTTTCACTTCTTCAAACCCACCAAAGGCAAAAGTAAATGCTGCTGGAGTGGTTGA
LMRG_01542	AGGTGTAGCAGAAGGAACAGCAAATATTACTGTCGCATCTA
	GATGGGTCAGATAACACCGAAGAGCAAGGCGATTATGACGGTGATGGCAACGAAAAA
LMRG_01541	ACGGTTGTGCTAGGTTACTCAGAAGCTTACACATTCGAAGGGA
	GAAATTAAGAACAGCGATATTAAAACCTGAATCGATTGCTTTGCTACTGACTCCAAATA
LMRG_01540	ACGCCAAACAAGGTTATCAAGACGGCTCTTATGAGCGGTCT
	CCGATTAAAGTACGTGTAGACCTCTCGAAAGCAAAAGGGAGCGTAAAAAAGGCGAAA
LMRG_01539	GAAAGAGGTCAGTTTGCTTTAATTAACCAAGCGGCTGCGGATA
	CAAATCGCGGGATTATCTGATAGTGATAGATATGATGCGGTTATTTTTATTGATGCAGT
LMRG_01538	GAATAGTATGAACGTGCCAGATAACTTTATAAGTAGATCTA
	TACAGTTAGCTACTTGTAATCAAATCGAGTATTTCAAAGAGGCTGGCGGAACAAGTGA
LMRG_01537	GTTAGCTGTTTCTAAGCCGGATAACGTATCAATCGGAAGAAC
	AACGAACTTGCGGCGGTCATTTCAGGAGACGACCCTTTAGACGCTTTAATGGGCAAAA
LMRG_01536	TCGCTTCTTGGTGGATGCGTCGAGAGCAAACTGTACTAATTT
	ACGGTAAGGACATTACAGCTGCTAAACAACAATTATCTGAGGTGGAAGCAGAGAGAG
LMRG_01535	ATGGCTTAAAAAGCCAGCTAACACAACGGGACAAAGATATTGA
	CGCTTGTGGATAAAGCTAATAAGCGATGGACGCCGGAATCATACGTTAAAACAGTAAC
LMRG_01534	TAGGACAACCGTCAACAGCGTTTATAACAGCATTGAAGACGA
	TGTTAAAACGGCTGTTAACCTAGACGGCTCAACCACGCAGTATTTCGATTCAACTGATG
LMRG_01533	AAGCATTCTTTTTATATCAAGGTGACCAAGACGACAACGGC

Table S4: continued

	AGTCGCCAATGGAAATTGTCCACAAAACTTGGGGGACAGGCTTCTATTTCTCTGGTTGT
LMRG_01532	GATGATCCCGCTAAACTAAAATCGATGAAAATTCCAGTCGG
	ACGATTTGCGGATGAATATATAAAATGCGGTAATGCTACAGAAGCCGCTCGCTTGGCT
LMRG_01531	GGTTATAGTTTGAAAACGGCTAATCGTATAGCGACCGAAAAC
	GCTAGTATAGATGAGTTGGAAATATACGAAGCCATTATAAAAAAACACAGTATATCAG
LMRG_01530	ATTCTAAAGTGAAGACCCAGTTGGAAAAATACAGAATAAGCA
	TATGATGATATAGCAGGAGATTGCTATGTTGCCCGGCAGAGGCTTTGTATCTGGCCACT
rliG	AGTCTCAACAGATGACGACACTTCTGTTCAATCTCATATCC
	TCAAAAGTAGAAGATGCTGCAATTCATAATGTCGATAACGTTCATGCAGCACAAGAAG
LMRG_01529	CGGTTAAAAAATACGATGCTATTTTGAATCAGCTTGAGCACA
	TGGGAAATGATTTCTTCACAACAGAGCCACCCCTTAATTGTGACTTAATGATTAGTAAC
LMRG_02921	CCGCCTTTTTCACAACAAAACGAAATAATAGAGCGTAGTTT

* presenting only probes that worked experimentally (52 in total)

Table S5. ϕ10403S transcriptional response during active lysogeny. Related to Figure 3.
Gene Expression Data Analysis generated by nSolver Analysis Software 4.0

Gene	RQ relative to lysogeny		
	Intracellular 2h vs. Log phase	Intracellular 4h vs. Log phase	Intracellular 6h vs. Log phase
LMRG_01511	0.93	0.57	0.59
LMRG_01512	1.10	0.99	0.6
LMRG_01513	1.39	1.13	0.74
LMRG_01514	1.59	1.5	1.46
LMRG_01515	1.78	2.19	6.82
LMRG_1516	1.91	2.25	6.69
LMRG_1517	1.78	1.96	6.06
LMRG_01518	1.82	2.08	6.53
lasRNA	0.47	0.19	0.15
LMRG_2984	2.28	1.87	5.58
LMRG_02920	1.83	1.65	4.85
LMRG_01521	1.71	1.58	5.48
LMRG_01522	1.76	1.65	5.62
LMRG_01523	1.62	1.68	6
rli140	2.29	2.42	7.74
LMRG_01524	1.75	1.51	5.3
LMRG_01525	1.53	1.23	4.74
LMRG_01526	1.82	1.47	5.72
LMRG_01527	1.87	1.46	5.79
LMRG_02921	2.39	1.82	5.97
LMRG_01529	1.82	1.36	5.64
rliG	0.78	0.54	1.23
LMRG_01530	2.26	1.94	3.86
LMRG_01531	2.37	0.79	1.21
LMRG_01532	2.13	0.73	1.04
LMRG_01533	1.96	0.49	0.76
LMRG_01534	1.90	0.43	0.81
LMRG_01535	0.91	0.22	0.32
LMRG_01536	0.91	0.2	0.26
LMRG_01537	0.92	0.21	0.29
LMRG_01538	0.89	0.21	0.24
LMRG_01539	0.92	0.22	0.31
LMRG_01540	0.91	0.22	0.27
LMRG_01541	0.94	0.22	0.27
LMRG_01542	1.01	0.24	0.36
LMRG_01543	0.96	0.25	0.32
LMRG_01544	1.11	0.3	0.41
LMRG_01545	1.30	0.35	0.67
LMRG_01546	1.26	0.38	0.63
LMRG_01547	1.49	0.46	0.72
LMRG_01548	2.03	0.61	1.05
LMRG_01549	1.59	0.5	0.89
LMRG_01550	1.43	0.54	0.98
LMRG_01551	1.37	0.43	0.63
LMRG_01552	1.37	0.4	0.62
LMRG_01553	1.16	0.39	0.64
LMRG_01554	1.56	0.49	0.73
LMRG_01555	1.82	1.99	1.63
LMRG_01556	2.26	2.13	1.74
LMRG_01557	1.61	1.78	1.08
LMRG_01558	14.10	15.85	21.69

Table S6: List of strains and mutants used in this study. Related to all Figures

Strain	Description
XL-1 blue	*recA1 endA1 gyrA96 thi-1 hsdR17 supE44 relA1 lac* [F' *proAB lacIqZΔM15 Tn10* (*TetR*)]
SM-10	Conjugation donor; F-*thi*-1 *thr*-1 *leuB6 recA tonA21 lacY1 supE44 (Muc*+) λ-[*RP4-2*(*Tc::Mu*)] *Kan*^{R} *Tra*+
Lm 10403S	*Listeria monocytogenes* Wild Type, Strp^R (WT)
Bs PY79	*Bacillus subtilis* PY79 Wild type (AES101)
Δϕ	*Lm* 10403S cured of ϕ10403S (Cured strain) DPL-4056
Δ*comK*	*Lm* 10403S deleted of *comK* gene and cured of ϕ10403S
Bs-amyE::Phs-llgA-terS	*Bs* PY79 *amyE::Phs-RBS5-llgA-terS-spec*
WT-pPL2-*cI*-like	*Lm* 10403S harboring pPL2 integrative plasmid constitutively expressing ϕ10403S CI-like repressor (*LMRG_01514*) under Pconst promoter (Argov et al., 2017b)
Δ*LMRG_01511*	*Lm* 10403S Δ*LMRG_01511* (Rabinovich et al., 2012)
Δ*LMRG_01512*	*Lm* 10403S Δ*LMRG_01512*
Δ*LMRG_01513*	*Lm* 10403S Δ*LMRG_01513*
Δ*LMRG_02918*	*Lm* 10403S Δ*LMRG_02918*
Δ*LMRG_01515*	*Lm* 10403S Δ*LMRG_01515*
Δ*LMRG_01516*	*Lm* 10403S Δ*LMRG_01516*
Δ*LMRG_01517*	*Lm* 10403S Δ*LMRG_01517*
Δ*LMRG_01518*	*Lm* 10403S Δ*LMRG_01518*
Δ*LMRG_02984*	*Lm* 10403S Δ*LMRG_02984*
PlasRNA	*Lm* 10403S harboring a mutated -10 site (GCTATAA→ AGAGTAA) in the *lasRNA* promoter
Δ*LMRG_02920*	*Lm* 10403S Δ*LMRG_02920*
Δ*LMRG_01521*	*Lm* 10403S Δ*LMRG_01521*
Δ*LMRG_01522*	*Lm* 10403S Δ*LMRG_01522*
Δ*LMRG_01523*	*Lm* 10403S Δ*LMRG_01523*
Δ*LMRG_01524-25*	*Lm* 10403S Δ*LMRG_01524* and *LMRG_01525*
Δ*LMRG_01525*	*Lm* 10403S Δ*LMRG_01525*
Δ*LMRG_01526*	*Lm* 10403S Δ*LMRG_01526*
Δ*LMRG_01527*	*Lm* 10403S Δ*LMRG_01527*
Δ*LMRG_02921*	*Lm* 10403S Δ*LMRG_02921*
Δ*LMRG_01528*	*Lm* 10403S Δ*LMRG_01528*
Δ*LMRG_01529*	*Lm* 10403S Δ*LMRG_01529 (llgA)*
Δ*rliG*	*Lm* 10403S Δ*rliG*
Δ*LMRG_01530*	*Lm* 10403S Δ*LMRG_01530*
Δ*LMRG_01531*	*Lm* 10403S Δ*LMRG_01531*
Δ*LMRG_01535*	*Lm* 10403S Δ*LMRG_01535*
Δ*LMRG_01551*	*Lm* 10403S Δ*LMRG_01551*
Δ*LMRG_01552*	*Lm* 10403S Δ*LMRG_01552*
Δ*LMRG_01553*	*Lm* 10403S Δ*LMRG_01553*
Δ*LMRG_01554*	*Lm* 10403S Δ*LMRG_01554*
(*lysis*)ϕ	*Lm* 10403S Δ*LMRG_01552, LMRG_01553* and *LMRG_01554*
Δ*LMRG_01555-56*	*Lm* 10403S Δ*LMRG_01555* and *LMRG_01556*
Δ*LMRG_01557*	*Lm* 10403S Δ*LMRG_01557*
Δ*LMRG_01558-9*	*Lm* 10403S Δ*LMRG_01558* and *LMRG_01559*
WT-pPL2-PactA-*llgA*	*Lm* 10403S harboring pPL2 integrative plasmid expressing *llgA* (*LMRG_01529*) under the promoter of the *actA* gene
Δϕ-pPL2-PactA-*llgA*	*Lm* 10403S Δϕ (Cured strain) harboring pPL2 integrative plasmid expressing *llgA* (*LMRG_01529*) under the promoter of the *actA* gene
(*lysis*)ϕ-pPL2-PactA-*llgA*	*Lm* 10403S (*lysis*)ϕ harboring pPL2 integrative plasmid expressing *llgA* (*LMRG_01529*) under the promoter of the *actA* gene
WT-pPL2-P*tetR-llgA-his*	*Lm* 10403S harboring pPL2 integrative plasmid expressing *llgA* (*LMRG_01529*) tagged with C'-6His under the *tetR* inducible promoter
Δϕ-pPL2-P*tetR-llgA-his*	*Lm* 10403S Δϕ (Cured strain) harboring pPL2 integrative plasmid expressing *llgA* (*LMRG_01529*) tagged with C'-6His under the *tetR* inducible promoter
(*lysis*)ϕ-pPL2-P*tetR-llgA-his*	*Lm* 10403S Δ*LMRG_01552-01554* harboring pPL2 integrative plasmid expressing *llgA* (*LMRG_01529*) tagged with C'-6His under the *tetR* inducible promoter
WT-ϕ*pheS*Km*	*Lm* 10403S with *pheS** (mutated phenylalanyl-tRNA synthetase) and Kanamycin resistance gene inserted in the ϕ10403s genome downstream to *LMRG_01556* (Argov et al., 2017b)
LMRG_01526-ϕ*pheS*Km*	*LMRG_01526* with *pheS** (mutated phenylalanyl-tRNA synthetase) and Kanamycin resistance gene inserted in the ϕ10403S genome downstream to *LMRG_01556*